Title

The catheterized bladder environment promotes Efg1- and Als1-dependent Candida albicans infection

Journal

Science Advances, 9(9)

ISSN

2375-2548

Authors

La Bella, Alyssa Ann

Andersen, Marissa Jeme

Gervais, Nicholas C

et al.

Publication Date

2023-03-03

DOI

10.1126/sciadv.ade7689

MICROBIOLOGY

The catheterized bladder environment promotes Efg1- and Als1-dependent *Candida albicans* infection

Alyssa Ann La Bella[1], Marissa Jeme Andersen[1], Nicholas C. Gervais[2], Jonathan Jesus Molina[1], Alex Molesan[1], Peter V. Stuckey[1], Lauren Wensing[2], Clarissa J. Nobile[3,4], Rebecca S. Shapiro[2], Felipe Hiram Santiago-Tirado[1]*, Ana Lidia Flores-Mireles[1]*

Catheter-associated urinary tract infections (CAUTIs) account for 40% of hospital-acquired infections (HAIs). As 20 to 50% of hospitalized patients receive catheters, CAUTIs are one of the most common HAIs, resulting in increased morbidity, mortality, and health care costs. *Candida albicans* is the second most common CAUTI uropathogen, yet relative to its bacterial counterparts, little is known about how fungal CAUTIs are established. Here, we show that the catheterized bladder environment induces Efg1- and fibrinogen (Fg)–dependent biofilm formation that results in CAUTI. In addition, we identify the adhesin Als1 as the critical fungal factor for *C. albicans* Fg-urine biofilm formation. Furthermore, we show that in the catheterized bladder, a dynamic and open system, both filamentation and attachment are required, but each by themselves are not sufficient for infection. Our study unveils the mechanisms required for fungal CAUTI establishment, which may aid in the development of future therapies to prevent these infections.

INTRODUCTION

Candida albicans is one of few fungal species that can cause serious infection in immunocompromised individuals and immunocompetent people with implanted medical devices (*1*). Normally, *C. albicans* is part of the healthy human microbiota, asymptomatically colonizing the gastrointestinal (GI) tract, reproductive tract, oral cavity, and skin of most humans (*1*, *2*). However, dysbiosis in the host environment, such as alterations in host immunity, stress, or resident microbiota, can promote *C. albicans* colonization and overgrowth, leading to biofilm formation and infection (*1*). The World Health Organization recently released a priority list of fungal pathogens and listed *C. albicans* under the "critical priority group" for research and public health action, indicating the importance of understanding virulence and biofilm formation of this pathogen in infections such as catheter-associated urinary tract infections (CAUTIs) (*3*).

C. albicans produces highly structured biofilms composed of multiple cell morphologies: yeast, pseudohyphae, and hyphae (*4*, *5*). Hyphal formation, hyphae-specific gene expression, and biofilm formation are hallmarks of virulence, invasion, and immune evasion, resulting in tissue damage and invasive infection (*6*). *C. albicans* biofilm formation is initiated by the adherence of yeast cells to a surface, forming microcolonies, and is followed by proliferation of pseudohyphae and hyphae (*6*). Hyphal growth is triggered via numerous environmental signals including serum, neutral pH, and CO_2 and is controlled by master transcriptional regulators such as enhanced filamentous growth 1 (Efg1) (*7*). Biofilm maturation occurs when the hyphal scaffold is encased in an extracellular polysaccharide matrix (*8*), and the final step involves dispersion of yeast cells to seed planktonic infections or to establish biofilms at other locations in the surrounding environment (*6*).

These robust and highly structured biofilms often develop on implanted medical devices, allowing *C. albicans* to colonize urinary and central venous catheters, pacemakers, mechanical heart valves, joint prostheses, contact lenses, and dentures (*1*–*3*). Biofilm formation on these devices predisposes patients to bloodstream infections and can lead to invasive systemic infections of tissues and organs (*1*). *Candida* biofilm formation on devices poses a serious threat because they are more resistant to antifungal therapy and can evade protection from host defenses (*8*). Newer antifungal drug classes, such as the echinocandins, that target the β-1,3 glucan component of the cell wall have shown some efficacy against *C. albicans* biofilms (*2*); however, echinocandin-resistant *Candida* spp. have been recently emerging (*9*).

The 2016 National Healthcare Safety Network review found that *Candida* spp., specifically *C. albicans*, has become the second most prevalent uropathogen, causing 17.8% of CAUTIs (*10*). CAUTIs are the most common nosocomial infection, with more than 150 million individuals acquiring these infections per year (*11*). The use of catheters and subsequent infections are not limited to hospital settings. In nursing homes, 11.9% of residents use indwelling catheters (*12*), and ~50% of catheterized residents will experience symptomatic CAUTIs (*13*). Despite *Candida* spp. prevalence in CAUTIs, there are no studies available regarding the pathogenesis of *Candida* spp. during CAUTI, and the roles of host and fungal factors remain unclear (*10*, *14*).

Urinary catheterization causes dysbiosis of the bladder environment by compromising the urothelium, inducing inflammation, interfering with normal micturition (voiding), and disrupting host defenses in the bladder (*15*–*17*). The inflammation response caused by catheterization exposes epithelial receptors and recruits host factors that can be recognized by the pathogen, enabling microbial colonization and persistence within the urinary tract (*15*–*17*). Specifically, host clotting factor 1, fibrinogen (Fg), is released into

[1]Department of Biological Sciences, University of Notre Dame, Notre Dame, IN, USA. [2]Department of Molecular and Cellular Biology, University of Guelph, Guelph, ON, Canada. [3]Department of Molecular and Cell Biology, University of California, Merced, Merced, CA, USA. [4]Health Sciences Research Institute, University of California, Merced, Merced, CA, USA.
*Corresponding author. Email: afloresm@nd.edu (A.L.F.-M.); fsantiago@nd.edu (F. H.S.-T.)

the bladder to heal damaged tissues and prevent bleeding due to catheter-induced inflammation in both mice and humans (*18*, *19*). Because of the constant mechanical damage caused by the urinary catheter, Fg accumulates in the bladder and deposits onto the catheter, where it is exploited by uropathogens (*18*–*21*). In an ex vivo study, we showed that a *C. albicans* CAUTI isolate colocalizes with Fg on urinary catheters (*19*). This suggests that aspects of the catheterized bladder environment induce changes in *C. albicans* virulence programming, prompting us to study potential fungal factors for CAUTI pathogenesis.

Here, we characterized the growth, morphology, and biofilm formation in urine, as well as the ability to cause CAUTIs, of four *C. albicans* clinical and laboratory strains. We found that urine supported *C. albicans* growth, activated virulence by inducing hyphal formation, and enhanced Fg-dependent biofilm formation mediated by the transcriptional regulator Efg1. Furthermore, we found that catheter-induced inflammation, specifically Fg, is necessary for fungal colonization of the urinary tract and further demonstrated that Efg1-dependent hyphal formation is critical for CAUTI establishment. We identified that the Efg1-induced adhesin, agglutinin-like sequence 1 (Als1), is important for mediating Fg-fungal interactions in vitro and in vivo, and its expression is crucial for fungal CAUTIs. This suggests that the development of therapies that target the Als1-mediated fungal-Fg interactions could potentially be useful in the treatment of *C. albicans* CAUTIs.

RESULTS

C. albicans survival and growth in urine promotes hyphal formation

C. albicans can infect a wide range of regions within the human body including the oropharyngeal area, GI tract, intra-abdominal area, skin, genitals, and urinary tract, demonstrating its plasticity to survive and replicate in different host environments (*1*, *2*, *7*, *11*, *22*). Because *C. albicans* is a prominent CAUTI pathogen, we compared growth and morphology in nutrient-rich and restrictive urine conditions using the common clinical bloodstream isolate used in laboratories (SC5314) and three urinary clinical isolates [Pt62, Pt65, and percutaneous nephrolithotomy 1 (PCNL1) (*19*, *23*)] representing infections from different urinary catheter dwell times and urinary tract sites (Materials and Methods and table S1). Because hyphal formation is important for promoting disease, we used a hyphal defective double deletion mutant strain in the SC5314 background, *efg1*Δ/Δ*cph1*Δ/Δ, to test whether hyphal formation is important in the catheterized bladder environment (table S1). In addition, microenvironment conditions induce *C. albicans* morphological changes that are associated with virulence (*1*, *5*). *C. albicans* can exhibit different morphologies (*6*), including yeast, pseudohyphae, and hyphae (*5*). The hyphal morphology is associated with invasive growth and increased fungal virulence (*7*). Therefore, we also determined how the bladder environment affects *C. albicans*′ morphology.

For growth analysis, yeast extract peptone dextrose (YPD), a standard *C. albicans* growth medium, and brain heart infusion (BHI), a common isolation medium for clinical strains, were considered rich environments under both static and shaking conditions. Static growth was used to mimic the bladder environment, and shaking growth was used as a comparison with standard laboratory culture conditions. For restrictive environments, we used human urine grown statically, supplemented with 10% human serum, amino acids, bovine serum albumin (BSA), or Fg to mimic plasma protein extravasation in the catheterized bladder (*20*). Serum albumin and Fg were chosen because they are two of the most abundant host proteins on catheters retrieved from humans and mice, and it has been shown that other uropathogens use them as nutrient sources (*18*, *20*, *24*, *25*). Last, we used amino acids as a general nitrogen source. Samples were taken at 0, 24, and 48 hours to assess growth by enumeration of colony-forming units (CFUs) and morphology by fluorescent microscopy. As expected, *C. albicans* strains grew in higher densities in rich media with aeration, while growth in static rich media was similar to any urine condition (Fig. 1 and fig. S1). Growth in restrictive environments varied widely, but all strains were able to grow to some extent. Human serum promoted growth of all strains by 24 hours and of most strains by 48 hours. A subsequent decline was observed by 48 hours for Pt65 and SC5314, possibly because all nutrients were consumed rapidly (Fig. 1, B and D). BSA and amino acids moderately promoted growth in all strains (Fig. 1). Fg enhanced growth of all strains compared to urine alone (Fig. 1).

For morphology analysis, YPD and urine, with or without serum, were used as rich and restrictive environments, respectively. The YPD conditions served as negative and positive controls for filamentation with the absence or presence of serum, respectively (*26*, *27*). Cell morphology analysis was done by quantifying the percentages of yeast, pseudohyphal, or hyphal forms (Fig. 2 and table S2). All strains showed predominantly yeast morphologies in YPD medium, and YPD with serum induced pseudohyphal and hyphal morphologies in all strains, except Pt65 and SC5314 *efg1*Δ/Δ*cph1*Δ/Δ. Notably, our analysis showed that urine conditions promoted pseudohyphal and hyphal formation in all strains (Fig. 2, A to D, and table S2) except SC5314 *efg1*Δ/Δ*cph1*Δ/Δ (Fig. 2E and table S2). Pseudohyphal and hyphal morphologies were further induced when urine was supplemented with human serum in wild-type (WT) laboratory and clinical strains. This suggests that the catheterized environment triggers *C. albicans* to transition from the yeast to hyphal morphology.

Fg enhances *C. albicans* biofilm formation

During candidiasis, *C. albicans* pseudohyphal and hyphal formation, observed on catheters from patients with CAUTI (*14*, *23*) and rats (*28*, *29*), induces expression of virulence genes including adhesion factors (*4*, *6*). Furthermore, our ex vivo study showed that the *C. albicans* PCNL1 clinical isolate colocalized with Fg, a known binding and biofilm platform for diverse uropathogens (*18*, *19*, *24*, *30*, *31*). Together, this suggests that Fg may be an important factor promoting *C. albicans* CAUTI pathogenesis. Thus, we hypothesized that urine conditions induce factors responsible for Fg-binding and biofilm formation.

Biofilm formation was compared in rich (YPD and BHI) and restrictive (human urine) media and between BSA- and Fg-coated microplates (Fig. 3, A to E). At 48 hours, immunostaining was performed to assess fungal biofilm biomass (*32*). We found that Fg promoted biofilm formation of all strains under all conditions and was further enhanced by human urine (Fig. 3, A to D). SC5314 *efg1*Δ/Δ*cph1*Δ/Δ formed enhanced biofilms in rich media when coated with Fg but was unable to do so in urine, regardless of the coated surface (Fig. 3E). This suggests not only that filamentation is important for biofilm formation in urine environments but

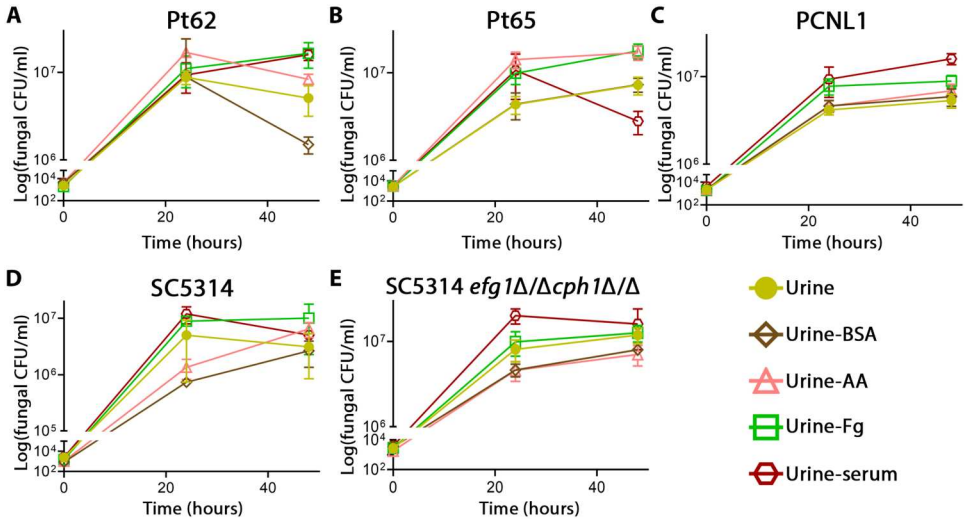

Fig. 1. *C. albicans* grows and survives in urine. (**A** to **E**) Growth curves of *C. albicans* strains Pt62 (A), Pt65 (B), PCNL1 (C), SC5314 (D), and SC5314 *efg1*Δ/Δ*cph1*Δ/Δ (E), grown in human urine conditions alone or urine conditions supplemented with 10% human serum (serum), Fg, BSA, or amino acids (AA). Fungal growth was determined by CFUs enumeration, and data are shown as log(fungal CFU/ml) after 0, 24, and 48 hours. Except when indicated, all strains were grown under static conditions. Data presented show the means and SEMs derived from three independent experiments with at least three technical replicates.

also that biofilm formation mechanisms differ between urine and rich environments.

Further analysis of biofilm formation was performed on *C. albicans* biofilms grown in urine on plates coated with either BSA, Fg, or fibrin meshes. Fibrin meshes were added because in damaged tissue environments such as the catheterized bladder, Fg is converted into fibrin fibers or meshes to stop bleeding and allow tissue healing (*33*). Visual examination of biofilm formation on BSA-, Fg-, or fibrin-coated plates showed that Fg- and fibrin-coated plates supported robust biofilm formation composed of yeast, pseudohyphae, and hyphae, while on BSA-coated plates, sparse monolayers or small aggregates of cells were observed (Fig. 3, F to I and K to N; see fig. S2 for zoomed-out images). However, SC5314 *efg1*Δ/Δ*cph1*Δ/Δ showed a small yeast-exclusive monolayer of cells regardless of BSA, Fg, or fibrin presence (Fig. 3, J and O; see fig. S2 for zoomed-out images). Together, this suggests that filamentation is

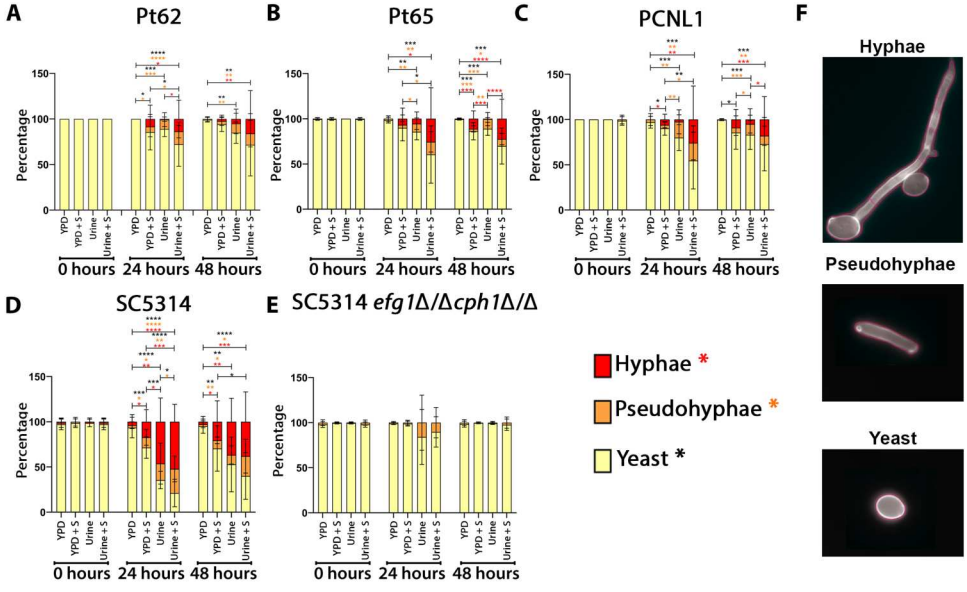

Fig. 2. Urine conditions induce *C. albicans*' transition to the hyphal morphology. (**A** to **E**) Morphology of *C. albicans* strains were evaluated after 0, 24, and 48 hours of growth in urine and YPD with or without 10% human serum. Images (consisting of a 3 × 3 tiled region, i.e., nine fields of view) were randomly acquired, and at least three images were analyzed per condition. The total number of cells per phenotype was summed and divided by the total number of cells, and the data are shown as overall percentage (%) of yeast, pseudohyphae, and hyphae (**F**). Differences between groups were tested for significance using the Mann-Whitney *U* test. **P* < 0.05, ***P* < 0.005, ****P* < 0.0005, and *****P* < 0.0001. *P* value colors represent the comparison between the different populations: hyphae (red), pseudohyphae (orange), and yeast (black). S, serum.

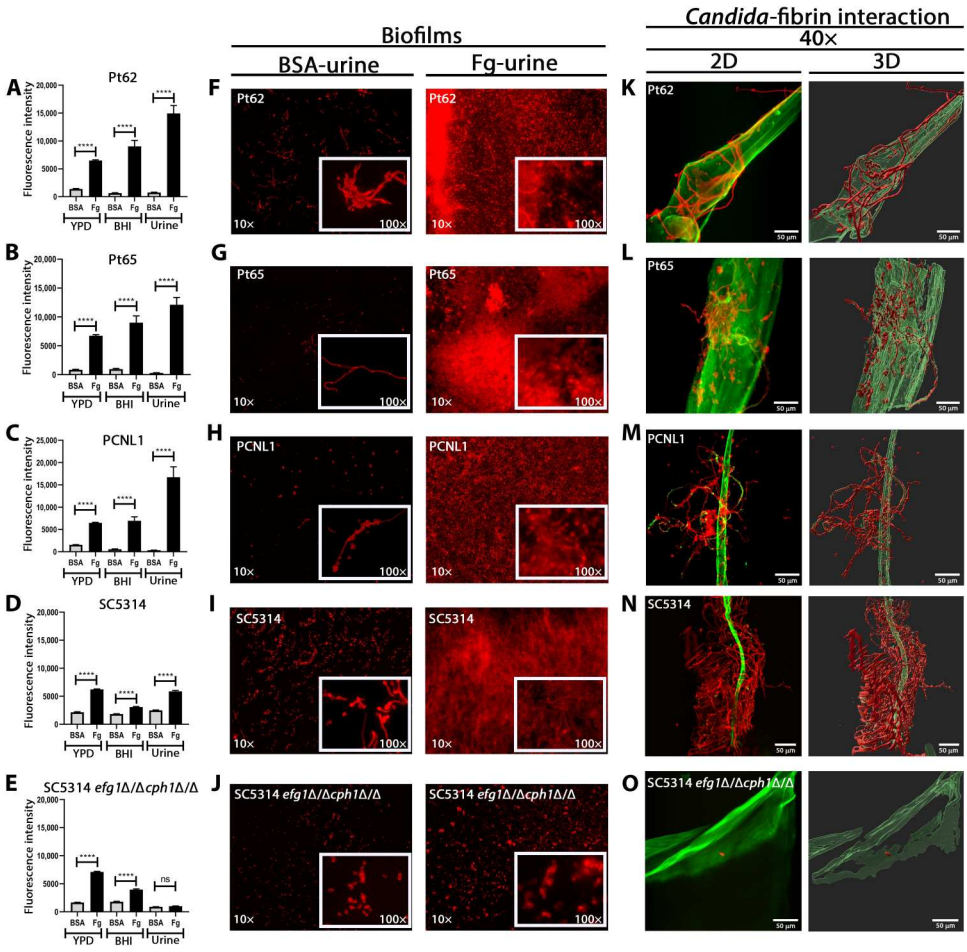

Fig. 3. Fg-fibrin interaction with *C. albicans* enhances biofilm formation. (**A** to **E**) Immunostaining analysis of biofilm formation on BSA- or Fg-coated microplates by *C. albicans* strains when grown in YPD, BHI, or human urine. At 48 hours, *C. albicans* biofilm formation was measured via fluorescence intensity using anti-*Candida* antibodies. Data presented show the means and SEs derived from three independent experiments with 24 technical replicates. Differences between groups were tested for significance using the Mann-Whitney *U* test. ****$P < 0.0001$; ns, not statistically different. (**F** to **J**) Microscopic visualization of 48-hour *C. albicans* biofilm biomass on BSA- or Fg-coated glass-bottom petri dishes grown in urine using anti-*Candida* antibodies. White squares represent the zoom-in area used for the higher magnification (×). (**K** to **O**) Microscopic visualization and three-dimensional (3D) reconstruction of 48-hour *C. albicans* biofilms on fibrin fibers/meshes grown in human urine using antibodies against Fg (anti-Fg; green) and *C. albicans* (anti-*Candida*; red). Scale bars, 50 μm. The 10× zoomed-out images are available in fig. S2.

important for Fg- and fibrin-dependent biofilm formation and that the regulation of Fg-binding adhesins expressed during hyphal morphogenesis is controlled by Efg1, *Candida* pseudohyphal regulator 1 (Cph1), or their downstream effectors.

C. albicans' hyphal formation and Fg interaction are critical for establishment of CAUTIs

On the basis of these results and the importance of biofilm formation for infections such as CAUTIs, we hypothesized that the *C. albicans* hyphal-deficient mutant strain would be unable to colonize the bladder and catheter. To test this hypothesis, we compared the ability of the clinical and laboratory strains to colonize the bladder both in the presence and absence of a catheter using our established mouse model (*18*, *20*, *24*, *25*, *30*, *31*, *34*, *35*). Mouse bladders were challenged with one of the strains, and 24 hours post-infection (hpi), the mice were euthanized, and fungal colonization was quantified via CFUs. Our results showed that catheterization significantly promoted bladder colonization by all the clinical and laboratory strains compared to the bladder colonization in noncatheterized mice (Fig. 4). Colonization by the hyphal-deficient mutant strain, SC5314 *efg1*Δ/Δ*cph1*Δ/Δ, was significantly impaired (Fig. 4D) and, in the absence of a catheter, behaved and colonized to the same extent as the WT strain. Because our mouse model of CAUTIs allows us to assess dissemination, we analyzed the fungal burden of the kidneys, spleen, and heart 24 hpi (Fig. 4). We found that urinary catheterization significantly contributed to fungal spread of SC5314 to the kidneys (Fig. 4D). Kidney colonization by Pt62 and Pt65 was 2 to 3 logs higher than noncatheterized mice, trending to significance (Fig. 4, A and B). The hyphal-deficient mutant strain, SC5314 *efg1*Δ/Δ*cph1*Δ/Δ, did not show differential dissemination between catheterized and noncatheterized mice (Fig. 4D).

To further understand *C. albicans*' morphogenesis, interaction with Fg, and spatial colonization in the bladder during CAUTIs, we performed histological analyses and immunofluorescence (IF) microscopy of catheterized bladders at 24 hpi. Bladder colonization

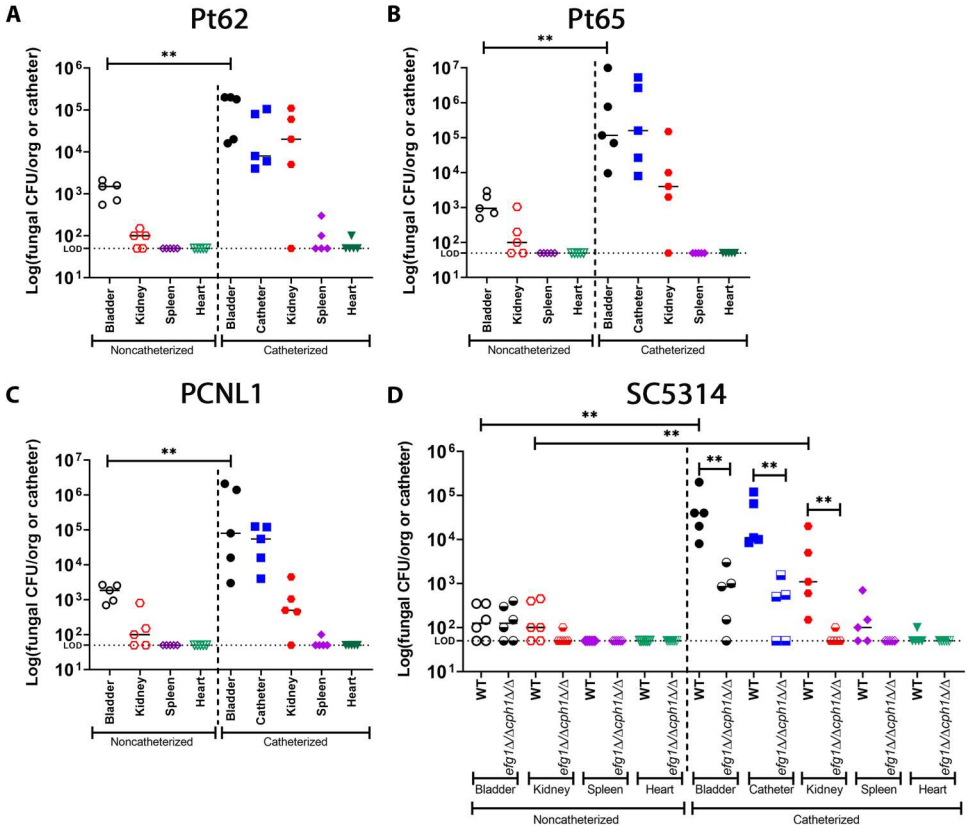

Fig. 4. Urinary catheterization promotes fungal colonization, and hyphal formation is required for CAUTI. (**A** to **C**) Fungal burden of clinical strains on the harvested organs and catheter. (**D**) Fungal burden comparison between laboratory strain SC5314 WT and SC5314 *efg1*Δ/Δ*cph1*Δ/Δ strains. Data are shown as the log(fungal CFU/org or catheter). The Mann-Whitney *U* test was used. **P* < 0.05 was considered statistically significant. ***P* < 0.005; ns, values were not statistically significantly different. The horizontal bar represents the median value. The horizontal broken line represents the limit of detection (LOD) of viable fungi. Infections were done in two independent experiments with *n* = 2 to 3 mice for each one. Animals that lost the catheter were not included in this work.

was exceptionally robust and was visible in the hematoxylin and eosin (H&E)–stained whole bladders (Fig. 5, blackarrowheads). Consistently, our IF analysis showed the presence of *C. albicans*' hyphal and pseudohyphal morphologies in the lumen of the bladder in all clinical and laboratory strains (Fig. 5, A to D), except the hyphal-deficient mutant strain, SC5314 *efg1*Δ/Δ*cph1*Δ/Δ (Fig. 5E). Furthermore, *C. albicans* cells in the catheterized bladder were found associated with Fg (Fig. 5; see figs. S3 to S7 for single channels). These data indicate that the changes induced by catheterization promote fungal colonization of the urinary tract and further demonstrate that hyphal morphogenesis and Efg1- and Cph1-regulated pathways are crucial for CAUTI establishment.

C. albicans interacts with Fg on the catheter surface in vivo during CAUTIs

On the basis of our in vitro Fg-binding results (Fig. 3), we assessed *C. albicans*–Fg interactions in vivo on the catheter during CAUTIs. Catheters from mice infected with each strain were retrieved 24 hpi, stained, and imaged. Except for the hyphal-deficient mutant strain, we found that all strains formed a robust biofilm on the implanted catheter [Fig. 5, G to K (merge images), and fig. S8 (single channels)], colonizing 59 to 79% of the surface of the catheter (table S3). SC5314 WT showed 78.9 ± 14% catheter colonization, while SC5314 *efg1*Δ/Δ*cph1*Δ/Δ showed 10.4 ± 7.5% catheter colonization, exhibiting a significant defect in colonization (Fig. 5O and table S3). Our IF analyses showed that *C. albicans* strains preferentially bound to deposited Fg on the catheters [Fig. 5, G to K, and fig. S8 (single channels)]. Quantification of the staining found that 75 to 91% of the *C. albicans* strains were colocalized with deposited Fg [Fig. 5, L to N, and fig. S8 (single channels)]. Although the hyphal-deficient strain was only able to colonize 10% of the catheter (Fig. 5O and table S3), its cells were colocalizing with Fg (Fig. 5K and table S3). This result further corroborates the importance of hyphal morphogenesis for biofilm formation and Fg for catheter colonization during CAUTIs.

Efg1 is critical for filamentation, Fg-dependent biofilm formation in urine, and the development of CAUTIs

We next explored the independent contributions of Efg1 and Cph1 to hyphal morphogenesis, Fg-dependent biofilm formation, and colonization of the catheterized bladder environment (Fig. 6 and fig. S9). Using single-deletion strains with their corresponding WT, we found that the *cph1*Δ/Δ strain produced pseudohyphae and hyphae similar to the WT strain, while the *efg1*Δ/Δ strain was predominantly in the yeast-form throughout all conditions (fig. S9). Fg-dependent biofilm formation was assessed, and the *cph1*Δ/Δ strain exhibited a ~40% decrease in biofilm formation when compared to the WT strains, while the *efg1*Δ/Δ strain showed a ~95%

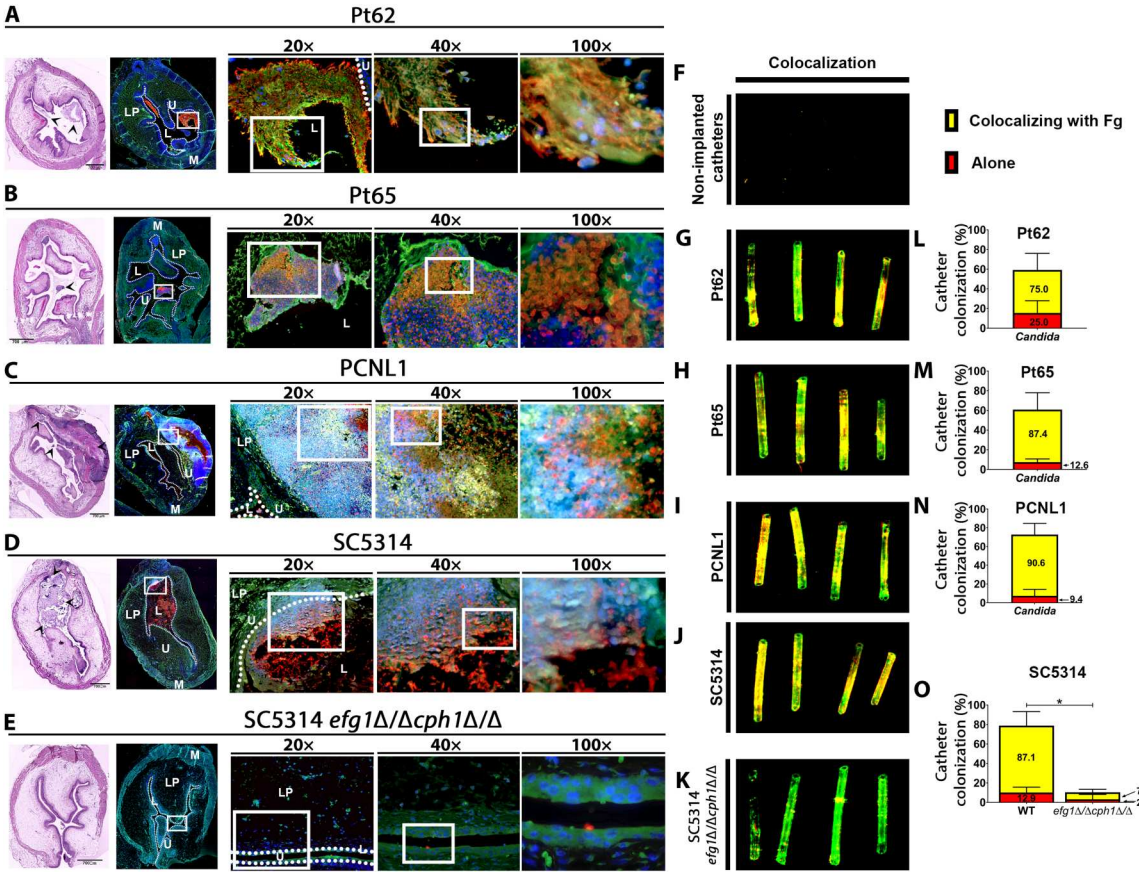

Fig. 5. Hyphal *C. albicans* cells invade the lumen of the catheterized bladder and interact with Fg on the bladders and catheters. (**A** to **E**) Implanted and infected bladders and catheters were recovered at 24 hpi. Bladders were subjected to analysis by H&E and IF staining. For the IF analysis, antibody staining was used to detect Fg (anti-Fg; green), *C. albicans* (anti-*Candida*; red), and neutrophils (anti-Ly6G; white). Staining with 4′,6-diamidino-2-phenylindole (DAPI; blue) delineated the urothelium and cell nuclei (representative images). The white broken line separates the bladder lumen (L) from the urothelium surface (U), the lamina propria (LP), and muscularis (M). H&E-stained bladder scale bars, 700 μm. White squares represent zoomed-in areas of higher magnification (20x, 40x, and 100x). Blackarrowheads indicate *C. albicans* colonization. (**G** to **K**) Implanted catheters were stained with antibodies to detect Fg (anti-Fg; green) and *C. albicans* (anti-*Candida*; red). The individual channels for each image are shown in figs. S3 to S7. Non-implanted catheters were used as negative controls (**F**). (**L** to **O**) Quantification of fungal (red) colocalization (yellow) with deposited Fg (green) on the catheter in percentage (%). The Mann-Whitney *U* test was used to analyze catheter colonization between SC5314 WT and hyphal mutant. **P* < 0.05. Values represent means ± SD derived from colocalization of the catheter segments. The individual channels for each image are shown in fig. S8.

reduction, and the *EFG1*-complemented strain restored biofilm formation to WT levels (Fig. 6A). Furthermore, analysis of fibrin interactions showed that the *cph1*Δ/Δ strain produced a robust hyphal colonization surrounding the Fg fibers, differing from the *efg1*Δ/Δ strain, which showed few yeast cells bound directly to the Fg mesh (Fig. 6B and fig. S2 for zoomed-out images). Analysis of colonization in our mouse model showed that the *efg1*Δ/Δ strain significantly impaired bladder and catheter colonization, while the *EFG1*-complemented and *cph1*Δ/Δ strains displayed comparable colonization to the WT strain (Fig. 6C). On the basis of the role of Efg1 in CAUTIs, *EFG1* expression levels were analyzed in the 24 hpi catheterized and infected bladders with WT, *efg1*Δ/Δ, and *EFG1*-complemented strains. We found that *EFG1* is expressed during bladder infection with the WT and *EFG1*-complemented strains and that *EFG1* transcripts were undetectable (ND) in the *efg1*Δ/Δ infected bladders as expected (fig. S10). Poor fungal dissemination of the spleen and hearts was observed (fig. S11A). Furthermore, analysis of bladder tissue showed that the *cph1*Δ/Δ strain–infected bladders had abundant hyphal burdens similar to the WT strain, while the *efg1*Δ/Δ strain–infected bladders showed defective colonization by sporadic yeast cells (Fig. 6D and figs. S12 to S14 for single channels). These phenotypes exhibited by the *efg1*Δ/Δ strain mimicked the phenotypes shown by the *efg1*Δ/Δ*cph1*Δ/Δ strain, indicating that Efg1 is the major transcriptional regulator responsible for the yeast-to-hyphal transition and for Fg-dependent biofilm formation in the catheterized bladder environment.

Neutrophils are highly recruited into the catheterized bladder (*20*, *25*, *36*) and neutropenic patients are more susceptible to *C. albicans* and bacterial dissemination originating from CAUTI (*37*, *38*). We next analyzed neutrophil recruitment into the catheterized and infected bladder via IF and flow cytometry. Imaging of bladders showed that neutrophils were highly recruited into the bladder, specifically in the areas with fungal colonization (Fig. 5 and figs. S3 to S7 for single channels). We also observed *C. albicans* cells breaching the urothelium where they encounter a strong neutrophil response (Fig. 5, C and D and figs. S5 to S6 for single channels). For example, PCNL1 was able to breach the bladder lamina propria, inducing

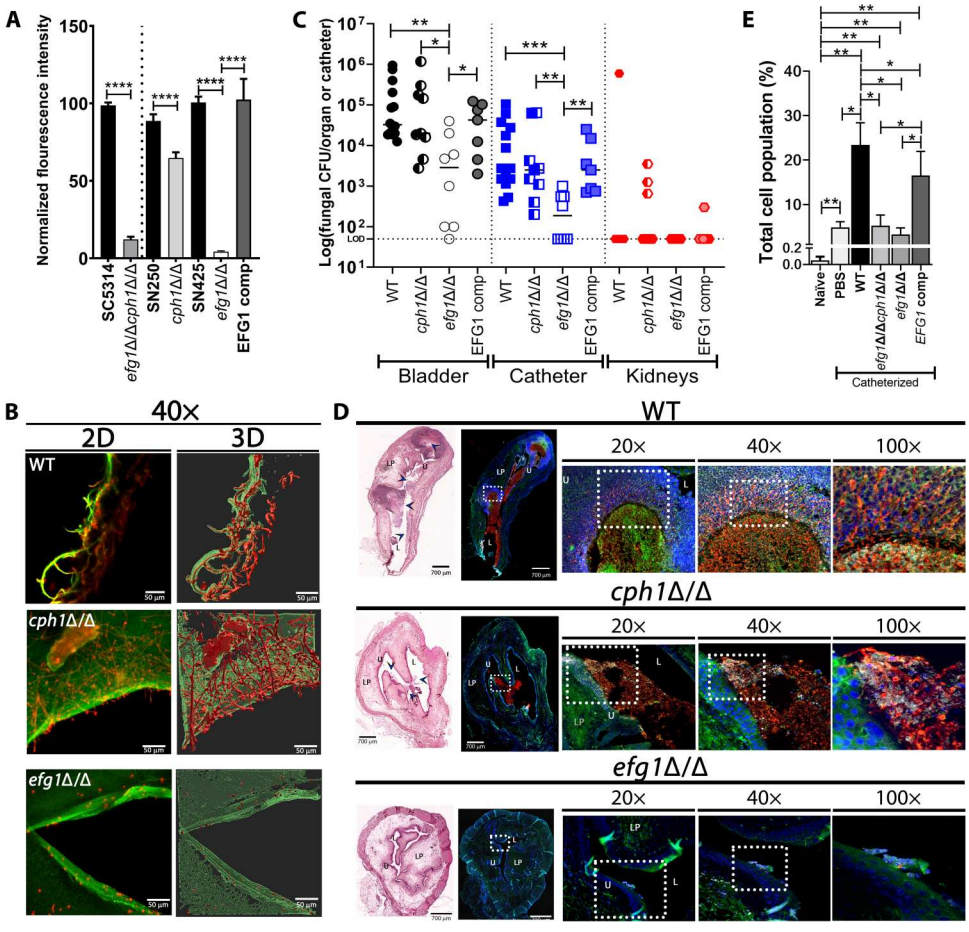

Fig. 6. Efg1 is responsible for inducing hyphal morphogenesis and is critical for establishment of CAUTI. (**A**) Comparison of biofilm formation on Fg-coated microplates by *C. albicans* strains when grown in urine for 48 hours. Quantification of fluorescence intensity normalized to the WT strain. (**B**) Microscopic visualization and 3D reconstruction of *C. albicans*-fibrin/mesh interaction grown in urine using antibodies against Fg (anti-Fg; green) and *C. albicans* (anti-*Candida*; red). Scale bars, 50 μm for 40x; the 10x magnification is in fig. S2. (**C**) Mice were catheterized and challenged with 1×10^6 CFUs of each strain, and burdens in bladder, kidneys, or catheters were quantitated as the number of CFUs [log(fungal CFU/organ or catheter)] recovered. For burden in other organs, see fig. S11. The horizontal broken line represents the limit of detection of viable fungi. Infections were done in three independent experiments with $n = 5$ mice for each one. Animals that lost the catheter were not included in this work. (**D**) Mouse bladders were harvested following infection and catheter implantation. Bladders were subjected to analysis by H&E and IF staining (anti-Fg, green; anti-*Candida*, red; anti-Ly6G, white; DAPI, blue). The individual channels for each image are shown in figs. S12 to S14. (**E**) Flow cytometry quantification of live neutrophils recruitment percentage (%) to the bladder in response of catheterization and infection. Representative gating strategy and flow plots are shown in fig. S15. Values represent means ± SEM. The Mann-Whitney *U* test was used; $P < 0.05$ was considered statistically significant. $^*P < 0.05$, $^{**}P < 0.005$, $^{***}P < 0.0005$, and $^{****}P < 0.0001$. The horizontal bar represents the median value.

massive neutrophil recruitment in attempt to contain the infection (Fig. 5C and fig. S5). Pt62 and Pt65 strains were primarily found in the bladder lumen, and their cells were interacting with Fg and neutrophils (Fig. 5, A and B, and figs. S3 to S4 for single channels). On the other hand, robust fungal colonization and neutrophil recruitment was not observed in the *efg1*Δ/Δ*cph1*Δ/Δ strain– or *efg1*Δ/Δ strain–infected bladders (Figs. 5E and 6D and figs. S7 and S14 for single channels). On the basis of these data, using flow cytometry, we quantified and compared bladder neutrophil recruitment in naïve and catheterized bladders that were phosphate-buffered saline (PBS)–mock infected or infected with the WT, *efg1*Δ/Δ*cph1*Δ/Δ, *efg1*Δ/Δ, and *EFG1*-complemented strains (Fig. 6E and fig. S15). We observed that the catheterized bladder by itself (PBS-mock infected) induced neutrophil recruitment; however, the infected bladder with the WT strain further increased neutrophil recruitment (Fig. 6E and fig. S15B), as we have observed via IF (Fig. 6D). Furthermore, neutrophil recruitment in the bladder infected with the *efg1*Δ/Δ*cph1*Δ/Δ and *efg1*Δ/Δ strains showed levels comparable to the PBS-mock–infected condition, while the *EFG1*-complemented strain was not significantly different from the WT strain (Fig. 6E and fig. S15B). These data demonstrate that in the catheterized bladder, infection with *C. albicans* leads to the recruitment of neutrophils to the site of infection, and the virulent hyphal and pseudohyphal morphologies are driven by Efg1.

Efg1 is also crucial for the pathogenesis of the *C. albicans* clinical strains

To confirm whether Efg1 is also critical for biofilm formation and establishment of *C. albicans* CAUTIs by the clinical strains, we first compared the *EFG1* expression levels in Fg-dependent biofilms

under urine and YPD conditions by quantitative reverse transcription polymerase chain reaction (qRT-PCR). We found that *EFG1* was significantly up-regulated in urine-grown biofilms when compared with those grown in YPD (Fig. 7A). On the basis of these data, we generated *EFG1* deletion strains in the clinical strain genetic backgrounds and compared their abilities to form Fg-dependent biofilms under urine conditions with that of their WT counterpart. We found that *efg1*Δ/Δ strains have a severe defect in biofilm formation when compared to the corresponding WT strains (Fig. 7B), confirming the importance of Efg1 in urine conditions. We further tested the *efg1*Δ/Δ strains in our mouse model of CAUTI, finding that colonization by *efg1*Δ/Δ strains was significantly decreased in the bladder and catheter (Fig. 7, C to E). These findings are similar to those observed for SC5314 *efg1*Δ/Δ*cph1*Δ/Δ and SC5314 *efg1*Δ/Δ colonization (Figs. 4D and 6C). These data indicate that Efg1 and its regulatory network are critical in diverse *C. albicans* strains for biofilm formation and establishment of colonization in the catheterized bladder environment.

An Efg1-regulated adhesin is critical for biofilm formation and fungal persistence during CAUTIs

We have demonstrated that *C. albicans* interacts with Fg, and its presence enhances colonization in the catheterized bladder (Figs. 3 to 4), suggesting that urine conditions induce the expression of Fg-binding adhesins. To identify adhesins important for attachment, colonization, and fungal persistence during CAUTIs, we screened 12 adhesin mutant strains from the Shapiro library (Fig. 8A) (*39*) and 27 adhesin and biofilm-related mutants from the Noble library (fig. S16A) (*40*) for Fg-dependent biofilm formation under urine conditions. We found that of all adhesin mutant strains, the *als1*Δ/Δ strain exhibited the most severe biofilm formation defect under urine conditions (Fig. 8A), similar to the biofilm defects of the *efg1*Δ/Δ and *efg1*Δ/Δ*cph1*Δ/Δ strains, without compromising hyphal morphology (Figs. 3E, 8A, and 6A and figs. S16 to S17). To confirm whether Als1 is important in the clinical strains during Fg-dependent biofilm formation, we compared the *ALS1* expression in biofilms grown in urine compared to those grown in YPD, finding that urine conditions induced *ALS1* up-regulation in all clinical strains (fig. S10C).

To further corroborate the role of Als1 in biofilm formation, we complemented *ALS1* in the *als1*Δ/Δ strain and found that the *ALS1*-complemented strain rescued biofilm formation to WT levels (Fig. 8B, *ALS1* comp). In addition, we assessed biofilm formation by an *ALS1* overexpression (*ALS1* OE) strain [obtained from the Shapiro laboratory (*41*)]. This strain not only rescued but also enhanced biofilm formation eightfold higher than the WT strain (Fig. 8B). Increased biomass was visible in the *ALS1* OE strain, and because of insufficient antibody penetration, crystal violet was used to assess biomass (fig. S16B). Visualization of the WT, *als1*Δ/Δ, and *ALS1* OE strain interactions with fibrin showed that the *als1*Δ/Δ strain displayed less attachment and colonization of the fibrin meshes, while the *ALS1* OE strain exhibited a more robust colonization than the WT strain (Fig. 8C).

We further compared the ability of the WT, *als1*Δ/Δ, *ALS1*-complemented, and *ALS1* OE strains to cause CAUTIs. The *als1*Δ/Δ strain displayed a significant defect in bladder and catheter colonization, while the colonization of the *ALS1*-complemented strain was similar to that of the WT; in addition, the *ALS1* OE strain showed a significant increase in bladder, catheter, and kidney colonization when compared to the WT strain (Fig. 8D). Furthermore, imaging of the *als1*Δ/Δ strain–infected bladders did not show fungal colonization (Fig. 8E), whereas the *ALS1* OE strain–infected bladders had abundant hyphal burdens similar to the WT strain [Fig. 8E and figs. S18 to S20 (single channels)]. Imaging of catheters found that the WT strain colonization covered ~92.4%, the *als1*Δ/Δ strain covered ~10.73%, and the *ALS1* OE strain covered ~87.5% of the catheter surfaces. Of that colonization, the fungal population colocalizing with deposited Fg was ~88.0% for the WT strain, ~93.0% for the *als1*Δ/Δ strain, and ~99.0% for the *ALS1* OE strain [Fig. 8, F and G, and fig. S21 (single channels)]. The residual binding to Fg in the *als1*Δ/Δ strain was similar to that of the *efg1*Δ/Δ*cph1*Δ/Δ strain, suggesting that this binding is mediated by other adhesins. Together, these data show that Als1 is induced by Efg1 and that Als1 is the Fg-binding protein critical for establishing colonization in the

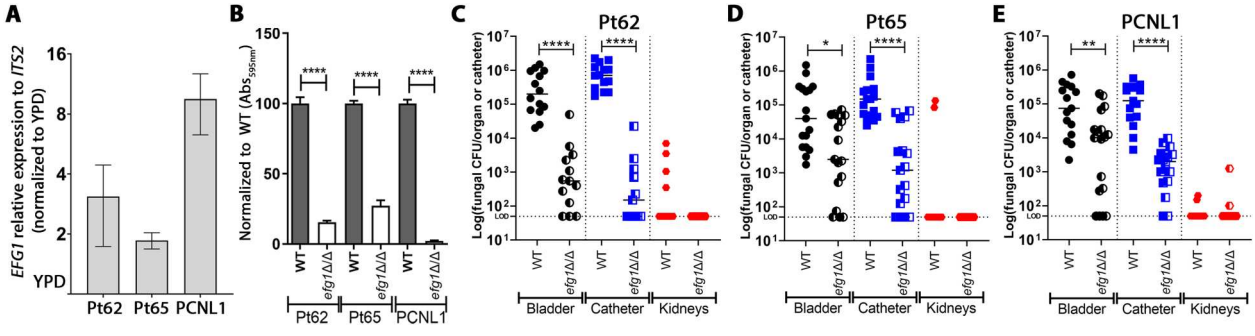

Fig. 7. Efg1 is important for *C. albicans* clinical strains during Fg-dependent urine biofilm and establishment of CAUTI. (**A**) Efg1 is expressed during Fg-dependent biofilms. For this, RNA was extracted from 48-hour biofilm in the clinical strains, and *EFG1* expression analysis was assessed by qRT-PCR. Data are shown as the relative expression normalized to the housekeeping gene, *ITS2*, and YPD. (**B**) Comparison of biofilm formation on Fg-coated microplates by *C. albicans* clinical strains WT and the corresponding *efg1*Δ/Δ mutant strain when grown in urine for 48 hours. Data are shown as the absorbance at 595 nm (Abs_{595nm}) normalized to WT values. (**C** to **E**) Colonization of organs and catheters by the clinical WT strains and their corresponding *efg1*Δ/Δ mutants. For burden in other organs, see fig. S11. The horizontal broken line represents the limit of detection of viable fungi. For CFU enumeration, infections were done in three independent experiments with $n = 5$ mice for each one, and data are shown as the log(fungal CFU/organ or catheter). Animals that lost the catheter were not included in this work. Values represent means ± SEM. The Mann-Whitney *U* test was used. $P < 0.05$ was considered statistically significant. *$P < 0.05$, **$P < 0.005$, and ****$P < 0.0001$. The horizontal bar represents the median value.

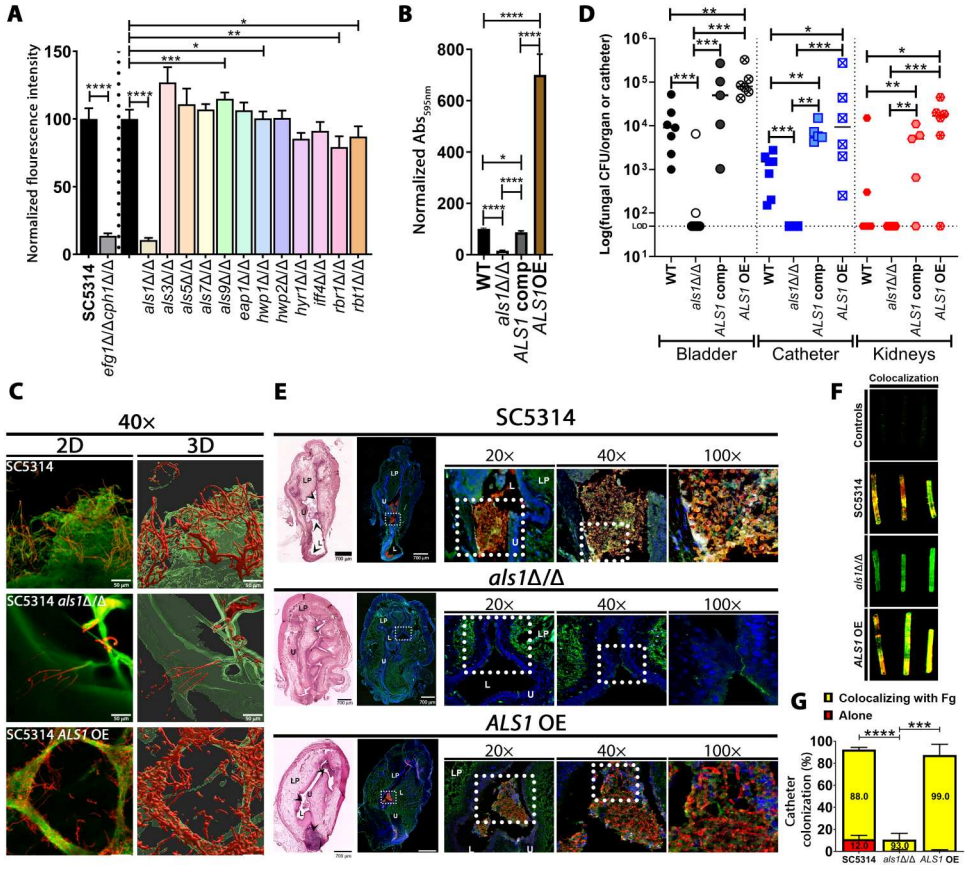

Fig. 8. Als1 is critical for Fg-dependent biofilm formation and establishment of CAUTI. Forty-eight–hour Fg-dependent urine biofilm formation analysis by *C. albicans* adhesin mutant strains (**A**) or the *ALS1* OE strain (**B**), measured via fluorescence intensity using anti-*Candida* antibodies (A) or crystal violet (B). Data are shown as fluorescence intensity normalized to WT values (A), or the absorbance at 595 nm normalized to WT values (B). Mean and SE are from three independent experiments with 24 technical replicates. (**C**) The 40× microscopic visualization and 3D reconstruction of *C. albicans* (red)–fibrin/meshes (green) interaction grown in urine (10× zoomed-out images are in fig. S2). (**D**) Fungal burden in the bladder, kidneys, or catheters at 24 hpi. For spleen and hearts burden, see fig. S11. The horizontal broken line represents the limit of detection. Two independent animal experiments were done with $n = 5$ mice for each, and data are shown as the log(fungal CFU/organ or catheter). Animals that lost the catheter were not included in this work. (**E**) H&E and IF analysis of catheterized and infected bladders. IF staining for detection of Fg (green), *C. albicans* (red), and neutrophils (white). DAPI (blue) was used to stain the cell nuclei. Bladder scale bars, 700 μm. White squares represent zoomed-in areas of higher magnification. Black-arrowheads on H&E indicate fungal bladder colonization; single channels are in figs. S18 to S20. (**F**) *C. albicans* (red) and Fg (green) colocalization in implanted catheters; single channels in fig. S21. (**G**) Fungal-Fg colocalization quantification on catheters. Data are shown as the percentage (%) of catheter colonization. The Mann-Whitney *U* test was used. *$P < 0.05$, **$P < 0.005$, ***$P < 0.0005$, and ****$P < 0.0001$.

catheterized bladder and that modulation of Als1 expression affects the outcome of infection.

Als1 has been reported to be an Efg1-downstream target (*42*). To confirm that Als1 regulation is dependent on Efg1 in the catheterized bladder, we analyzed *ALS1* expression levels in 24-hpi catheterized and infected bladders with either WT, *efg1*Δ/Δ, and *EFG1*-complemented strains (fig. S10B). We found that *ALS1* expression significantly decreased in bladders infected with the *efg1*Δ/Δ strain compared with bladders infected with the WT and *EFG1*-complemented strains (fig. S10B). This further suggests that Als1 is an Efg1-downstream effector in the catheterized bladder.

Als1 overexpression in the *efg1*Δ/Δ strain does not completely rescue its defective CAUTI colonization

Thus far, we have established that Efg1 and Als1 are essential factors for *C. albicans* virulence in the catheterized bladder. We found that *ALS1* expression significantly decreased in bladders infected with the *efg1*Δ/Δ strain compared with bladders infected with the WT and *EFG1*-complemented strains (fig. S10B). However, the *als1*Δ/Δ strain can still filament and form hyphae (Fig. 8C and fig. S17), indicating that Efg1 independently regulates both hyphal formation and Als1 expression. To distinguish the contributions of Efg1-hyphal morphology and adhesion during CAUTIs, we obtained a strain that overexpressed *ALS1* in the *efg1*Δ/Δ background (*efg1*Δ/Δ + p*ALS1*) and confirmed that *ALS1* is expressed during biofilm formation (Fig. 9A) and that *ALS1* overexpression did not induce hyphal formation (Fig. 9B) under urine conditions. We further evaluated whether *ALS1* overexpression could rescue the *efg1*Δ/Δ strain's defect in biofilm formation and found that *efg1*Δ/Δ + p*ALS1* partially rescued biofilm formation compared to the WT and *efg1*Δ/Δ strains (Fig. 9C). Last, we compared the ability of the WT and *efg1*Δ/Δ + p*ALS1* strains to cause CAUTIs. We found that *efg1*Δ/Δ + p*ALS1* did not completely rescue bladder and catheter colonization to WT level, showing significantly

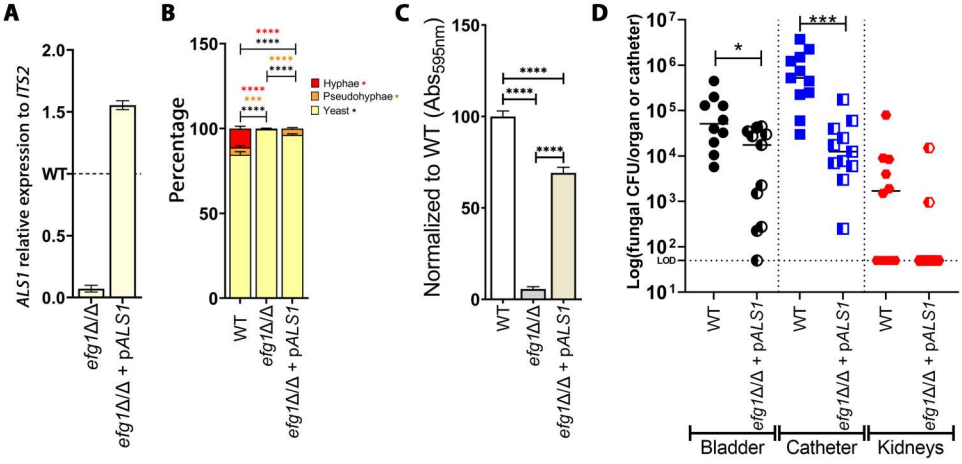

Fig. 9. Als1 overexpression in *efg1*Δ/Δstrain does not rescue its defective CAUTI colonization. (**A**) *ALS1* expression during 48-hour Fg-dependent biofilms by SC5314 WT, *efg1*Δ/Δ, and *efg1*Δ/Δ overexpression *ALS1* (*efg1*Δ/Δ + p*ALS1*). RNA was extracted from 48-hour biofilm in the clinical strains, and ALS1 expression analysis was assessed by qRT-PCR. Data are shown as the relative expression normalized to the housekeeping gene, *ITS2*, and WT. (**B**) SC5314 WT, *efg1*Δ/Δ, and *efg1*Δ/Δ + p*ALS1* morphologies were evaluated after 48 hours of growth in urine. Representative images were taken at ×100 magnification and processed with manual counting of yeast, pseudohyphae, and hyphae. Images (consisting of a 3 × 3 tiled region, i.e., nine fields of view) were randomly acquired, and at least three images were analyzed per condition. The total number of cells per phenotype were summed and divided by the total number of cells, and the data are shown as overall percentage (%) of yeast, pseudohyphae, and hyphae. (**C**) Biofilm formation analysis on Fg-coated microplates by SC5314 WT, *efg1*Δ/Δ, and *efg1*Δ/Δ + p*ALS1* strains when grown in human urine. At 48 hours, *C. albicans* biofilm biomass was measured with crystal violet. Data are shown as the absorbance at 595 nm normalized to WT values. (**D**) SC5314 WT and *efg1*Δ/Δ + p*ALS1* fungal burden in bladder, kidneys, or catheters at 24 hpi were quantitated as the number of CFUs recovered. For burden in other organs, see fig. S11. For CFU enumeration, infections were done in two independent experiments with $n = 6$ mice for each one, and data are shown as the log(fungal CFU/organ or catheter). Animals that lost the catheter were not included in this work. Differences between groups were tested for significance using the Mann-Whitney *U* test. *$P < 0.05$, ***$P < 0.0005$, and ****$P < 0.0001$. (B) *P* value colors represent the comparison between the different populations: hyphae (red), pseudohyphae (orange), and yeast (black).

decreased colonization (Figs. 6C and 9D). This suggests that Als1 is critical for colonization but that Efg1-driven pathophysiological processes, such as hyphal formation and virulence, are still required for *C. albicans* CAUTIs.

DISCUSSION

Candida spp. CAUTIs are increasing, most commonly in prolonged urinary catheterization and intensive care unit settings (*43*, *44*). Our results have shown that urinary catheterization significantly promotes colonization of the bladder by all strains to $\geq 10^5$ CFUs/ml, meeting the CDC's standard for UTI criteria (*45*), whereas in the absence of the catheter, colonization by all strains was significantly lower at $\leq 10^3$ CFUs/ml (Fig. 4). In this analysis, it is possible that colonization by filamenting strains is even higher than the CFU enumeration indicates because hyphal cells are highly multinucleated cells. Moreover, we observed that the clinical isolates, which were collected from patients with different catheterization times and sites of infection, exhibited higher burdens compared with the common bloodstream clinical isolate strain, SC5314. However, the urinary clinical isolate strains use the same mechanism as SC5314 because *EFG1* and *ALS1* are highly up-regulated in these strains during CAUTIs and deletion of *EFG1* renders them unable to cause infection (Fig. 7 and fig. S10). Regardless, our model indicates that the prevalence of *C. albicans* in the infected bladder is due to increased colonization, mediated by Efg1 and Als1, prompted by changes in the bladder environment that are caused by urinary catheterization (Figs. 4 and 7 to 9).

In this study, we also found that Efg1-dependent hyphal morphogenesis and Als1-mediated interactions with Fg and fibrin are critical for fungal CAUTI establishment (Figs. 6 to 9). Fg enhances *C. albicans* biofilm formation via interactions with the adhesin Als1. In addition, urine promotes Efg1 hyphal morphogenesis, which is essential for biofilm formation and infection during CAUTIs. *C. albicans* hyphal formation also induces strong neutrophil recruitment in the bladder to attempt to control the fungal infection. This causes further damage to the urothelium via migration of the neutrophils to the site of infection. Thus, the catheterized bladder creates the ideal environment for *C. albicans* to colonize and persist in the host.

Host proteins have been shown to contribute to fungal biofilm formation (*29*). We demonstrated that Fg is accumulated in the bladder and deposited on the catheters (*10*, *19*) and have seen that the *C. albicans* PCNL1 clinical isolate colocalized with Fg deposited on urinary catheters retrieved from a patient with preoperative negative urine culture (*19*). Moreover, a study from the Andes group showed that Fg and other host proteins were associated with *C. albicans* biofilms in urinary catheters retrieved from rats (*29*). Therefore, we focused on understanding the role of Fg in *C. albicans* CAUTIs. We found that hyphal formation was critical for Fg-dependent biofilm formation in urine conditions but not in YPD and BHI media, while the hyphal defective mutant strain was not able to form Fg-dependent biofilms in urine but could in rich media (Fig. 3). This seemingly contradictory result is not necessarily unexpected because we have observed that laboratory growth media does not fully recapitulate conditions found within the host. For example, several factors critical for bacterial biofilm formation in CAUTI are dispensable for in vitro biofilm formation when using conventional laboratory growth media (*18*, *25*). This difference could be related to adhesins that are expressed in the yeast cells

that may contribute to biofilm growth under laboratory conditions. Thus, using conditions that closely mimic the in vivo environment is important to identify physiologically relevant determinants for CAUTI colonization and survival.

To further mimic the bladder environment, we incorporated the presence of host proteins, BSA and Fg, into our in vitro studies. These proteins are found in the catheterized bladder because of the inflammation response caused by urinary catheter mechanical damage. Indubitably, we found that Fg enhances fungal biofilm formation in urine conditions and during urinary catheterization and that this is mediated by Als1 (Figs. 3 and 8 and fig. S16). *C. albicans* expresses numerous adhesion proteins, including the known Fg-binding protein 58kDa surface mannoprotein {Mp58 [pH regulated antigen 1 (Pra1) in SC5314]} (*46*); however, in urine conditions, Als1 is the primary adhesin of Fg. We found that modulation of Als1 affected the outcome of biofilm formation and infection, with the *C. albicans als1*Δ/Δ strain displaying defective Fg-dependent biofilm formation and in vivo colonization. Conversely, the *ALS1*-complemented strain and the *ALS1* overexpression strain rescued Fg-dependent biofilm formation and promoted CAUTI pathogenesis, while *ALS1* overexpression in the *efg1*Δ/Δ background showed only partial rescue of these phenotypes (Figs. 8 and 9). Previous structural studies showed that the N-terminal domain of Als1 interacts with Fg (*47*, *48*), binding to the Fg γ-chain via protein-protein interactions, similar to Clumping factor (Clf) adhesins in *Staphylococcus aureus* (*48*, *49*). Als1 belongs to the Als protein family of cell surface glycoproteins, which are important for adhesion to host, bacteria, and abiotic surfaces (*47*). Als3 and Als9-2 (an allelic variant of Als9) have been shown to interact with Fg (*47*, *48*); however, they are dispensable in Fg-dependent biofilm formation in urine (Fig. 8A). This may suggest that these factors are not expressed under urine conditions. Our results indicate that Als1 is an Efg1-downstream target in the catheterized bladder environment (fig. S10). Studies have shown that Efg1 also regulates *ALS3* expression under serum conditions (*50*) and that Efg1 directly binds to the *ALS3* promoter during biofilm formation in Spider media (*51*). Efg1 has both overlapping and distinct targets under different environmental conditions (*50*). Therefore, future studies dissecting the Efg1 regulatory network in the catheterized bladder will be crucial to understanding *C. albicans*' cellular signaling and to better manage the outcome of infection.

It has been established that urinary catheterization causes mechanical damage to the bladder, inducing epithelial wounding and triggering robust inflammation (*20*, *52*). In addition, clinical studies have detected *C. albicans* hyphae and biofilms on indwelling urinary catheters retrieved from patients with candiduria (*14*, *53*, *54*), suggesting fungal pathogenic activity during urinary catheterization. Here, we demonstrated that urine induces hyphal morphogenesis in vitro (Fig. 2 and table S2) and in vivo (Figs. 5, 6, and 8) and that Efg1-dependent hyphal programming is critical for bladder and catheter colonization (Figs. 6 and 7). Recently, deletion of epithelial escape and dissemination 1 (*EED1*) in *C. albicans* was shown to result in inhibition of hyphal formation but not virulence; this was attributed to the overexuberant growth of the *eed1*Δ/Δ strain (*55*). Because we observed invasive hyphal colonization in the catheterized bladder (Figs. 5, A to D, and 6D) and Als1-mediated Fg interactions are required for CAUTIs, we concluded that both filamentation and Als1 function are needed. In future experiments, the relationship between filamentation and CAUTIs can be explored in more detail using the *eed1*Δ/Δ strain to assess if it can cause CAUTIs, promote bladder tissue invasion and colonization, and induce a strong neutrophil response.

Furthermore, strong neutrophil recruitment during hyphal colonization (for the WT, *cph1*Δ/Δ, and *EFG1*-complemented strains) in the catheterized bladder was observed, whereas colonization with hyphal-deficient strains (*efg1*Δ/Δ*cph1*Δ/Δ and *efg1*Δ/Δ) showed similar neutrophil levels as the PBS-mock–infected bladders (Fig. 6, D to E). This observation is important because invasive fungi (largely in the hyphal form) evoke an active host immune and inflammatory response, while commensal fungi (largely in the yeast form) promote immune tolerance and "peaceful coexistence" with the microbiota (*56*). Our results strongly suggest that *C. albicans* has a pathogenic programming triggered by the catheterized bladder environment, resulting in fungal CAUTIs.

During CAUTIs, neutrophils are heavily recruited to the bladder as a defense mechanism against invading pathogens, and their numbers increase with extended catheterization (*20*, *36*). In neutropenic mice, the bacterial burden increases 10-fold during CAUTIs, suggesting that neutrophils are controlling and containing the infection in the bladder (*20*). Similarly, neutropenic patients developed candidemia from candiduria, suggesting that bladder recruited neutrophils are critical to controlling fungal systemic dissemination (*37*). Neutrophils have shown to be the major immune cells in the control of candidiasis (*57*) by phagocytizing and killing yeast cells and short hyphae, while longer hyphae are killed by inducing neutrophil extracellular traps, which release DNA, granule enzymes, and antimicrobial peptides (*58*). Our future studies will be focused on understanding the immune cell strategies against fungal CAUTIs and their roles in containing the fungal infection in the bladder.

C. albicans occupies many niches in the human body, and morphological changes are associated with the establishment of diseased states. This is important in the bladder because it is an open and dynamic system, where urine is constantly passing through. Therefore, to establish a successful colonization, adhesion and biofilm formation on the urinary catheter are essential (*18*, *31*). Our results are consistent with that; the *als1*Δ/Δ strain is able to form hyphae and small aggregates on fibrin nets (Fig. 8C), yet it is completely unable to cause CAUTIs (Fig. 8D), highlighting the importance of both filamentation and adhesion. This was further confirmed by testing the *efg1*Δ/Δ + p*ALS1* strain in our mouse model. While this strain was able to colonize by overexpression of *ALS1*, it was not fully able to recapitulate the bladder and catheter burden that we observed in the WT strain, emphasizing the importance of both filamentation and adhesion (Fig. 9). *Candida* biofilms not only ensure colonization but also protect the growing fungal cells from the hostile host environment and potentiate the establishment of the infection (*42*). This is the first study unveiling the *C. albicans* mechanism of pathogenesis during CAUTIs, finding that Efg1 and specifically its downstream target Als1 are critical for establishing infection (Fig. 10). This study opens avenues to understanding *C. albicans* cellular programming in the catheterized bladder. The key interaction of Als1-Fg, an initial step for colonization, could be exploited as a potential therapeutic avenue to prevent *C. albicans* CAUTIs.

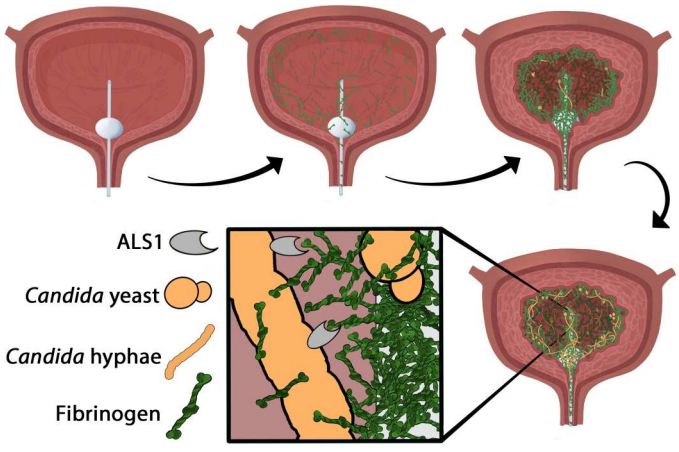

Fig. 10. *C. albicans* hyphal morphogenesis and Als1-Fg interactions are critical for CAUTI. Urinary catheterization results in mechanical damage to the bladder and leads to the release of Fg and its accumulation and deposition in the bladder and on the urinary catheter. The Fg-coated catheter serves as a scaffold for *C. albicans* attachment, leading to robust biofilm formation consisting of yeast, pseudohyphae, and hyphae. *C. albicans* attachment to Fg can be attributed primarily to the adhesin Als1. As a result of this adherence to Fg, *C. albicans* is able to persist in the bladder and establish CAUTI.

MATERIALS AND METHODS

Ethics statement

All animal care was consistent with the Guide for the Care and Use of Laboratory Animals from the National Research Council. The University of Notre Dame Institutional Animal Care and Use Committee approved all mouse infections and procedures as part of protocol number 18-08-4792MD. For urine and blood collections, all donors signed an informed consent form, and protocols were approved by the Institutional Review Board of the University of Notre Dame under study #19-04-5273 for urine and #18-08-4834 for blood.

Urine collection

Human urine from at least two healthy female donors between the ages of 20 to 35 were collected and pooled. Donors did not have a history of kidney disease, diabetes, or recent antibiotic treatment. Urine was sterilized with a 0.22-μm filter (VWR 29186-212), and pH was normalized to 6.0 to 6.5. BSA (VWR 97061–48)–supplemented urine was sterilized again using a 0.22-μm filter. When urine was supplemented with Fg (Enzyme Research Laboratories FIB 3), it was added directly to the sterilized urine, and the urine was not sterilized after the addition of Fg.

Fungal cultures

All strains of *C. albicans* were cultured at 37°C with aeration in 5 ml of YPD [yeast extract (10 g/liter; VWR J850-500G), peptone (20 g/liter; VWR J636-500G), and dextrose (20 g/liter; VWR BDH9230-500G)] broth. For in vivo mouse experiments, *C. albicans* strains were grown static overnight in 10 ml of YPD. The selection of the urinary clinical strains tested in this study was based on high fungal burden during isolation (~10^6 to 10^8 CFU/ml) and infections developed at different time points and urinary tract sites. Pt62 was recovered from a patient that had a catheter for 1 day. Pt65 was recovered from a patient that had a catheter for 6 days. PCNL1 is a kidney stone clinical isolate from a catheterized patient with a *C. albicans* kidney infection.

Generation of *C. albicans* CRISPR plasmids

The CRISPR plasmids for genetic manipulation of *C. albicans* were generated as previously described [(*41*) for CRISPRa and (*59*) for CRISPR knockouts]. Briefly, for CRISPR *EFG1* knockouts, a gene block was cloned into the pRS252 backbone (*C. albicans*–optimized CRISPR plasmid) via Gibson assembly. The gene block was synthesized by Integrated DNA Technologies and contains two single guide RNAs single guide RNAs (sgRNAs), the *SNR52* sgRNA promoter, regions of homology upstream and downstream of the *EFG1* open reading frame (ORF), and regions of homology for Gibson assembly. For this construct, two independent sgRNAs were designed and synthesized that flank the ORF of the *EFG1* gene. For Gibson assembly, the plasmid was digested with NgoMIV and combined with the synthesized gene block fragment (50 ng/μl) and NEBuilder 2x Hifi DNA Master Mix, for a total volume of 6 μl, and incubated at 50°C for 4 hours. For the CRISPRa *ALS1* plasmid, a sgRNA crispr RNA (crRNA) N20 sequence targeting the promoter region of *ALS1* was cloned into the dCas9-VPR CRISPRa plasmid (pRS156) via Golden Gate cloning at the Sap I locus, as previously described in detail (*41*). The assembled plasmid was transformed into chemically competent *Escherichia coli* DH5α.

C. albicans transformation

C. albicans cells were transformed as previously described in detail (*59*). Briefly, the plasmids were miniprepped and linearized with Pac I to allow plasmid integration at the *C. albicans NEUT5L* locus. The linearized plasmid and *C. albicans* cells were incubated with 800 μl of 50% polyethylene glycol, 100 μl of 10× tris-EDTA buffer, 100 μl of 1 M lithium acetate (pH 7.4), 40 μl of salmon sperm DNA, and 20 μl of 1 M dithiothreitol (DTT) and incubated at 30°C for 1 hour and at 42°C for 45 min. Cells were grown in YPD medium for 4 hours at 30°C with shaking, and transformants were selected on YPD agar plates with nourseothricin (250 μg/ml; NAT) and restreaked onto fresh YPD + NAT plates. *C. albicans*–transformed colonies were PCR-verified for the presence of the Cas9/dCas9 construct and either the *ALS1* guide sequence or the *EFG1* deletion.

Growth curves

Growth curves were performed in glass test tubes (Thermo Fisher Scientific, 14-961-29). Overnight cultures (all in stationary phase; measured using an ultraviolet-visible spectrophotometer) were normalized to ~1 × 10^6 CFU/ml in 1× PBS (Sigma-Aldrich, 1002786391). The culture was then diluted (1:1000) into human urine [supplemented with BSA (1 mg/ml), Fg (1 mg/ml), 50× amino acids, or human serum (1 mg/ml)], BHI (incubated statically or shaking), or YPD (incubated statically or shaking) and were incubated in the test tube at 37°C for 48 hours. At 0, 24, and 48 hours, samples of each condition were taken and analyzed by CFU counts.

Morphology assay and analysis

All strains of *C. albicans* were grown in YPD with or without serum and in human urine with or without serum. At 0, 24, and 48 hours, a sample of each condition was taken, fixed with 10% formalin, and stained with calcofluor (100 μg/ml). Samples were viewed under a Zeiss inverted light microscope (Carl Zeiss, Thornwood, NY) with

the 4′,6-diamidino-2-phenylindole fluorescent channel. Random images were taken at 100× magnification and processed with manual counting of yeast, pseudohyphae, and hyphae. Images (consisting of a 3 × 3 tiled region, i.e., nine fields of view) were randomly acquired, and at least three images were analyzed per condition. The total number of cells per phenotype were summed and divided by the total number of cells to give the overall percentage of each cell type.

The following primary antibodies were used: goat anti-Fg (Sigma-Aldrich, F8512), rabbit anti-*Candida* (Thermo Fisher Scientific, PA1-27158), and rat anti-mouse lymphocyte antigen 6 complex locus [Ly6G (BD Pharmingen, 551459)]. The following secondary antibodies were used: Alexa Fluor 488–labeled donkey anti-goat (Thermo Fisher Scientific, SA5-10086), Alexa Fluor 594–labeled donkey anti-rabbit (Thermo Fisher Scientific, SA5-10039), Alexa Fluor 647–labeled donkey anti-rat (Thermo Fisher Scientific, SA5-10029), IRDye 800CW donkey anti-goat, and IRDye 680LT donkey anti-rabbit. Alexa Fluor secondary antibodies were purchased from Invitrogen Molecular Probes, and IRDye conjugate secondary antibodies were from LI-COR Biosciences. The following dyes were used: calcofluor white (Fluorescent Brightener 28; Sigma-Aldrich, F3543) staining, Hoechst dye (Thermo Fisher Scientific, 62249) staining, and H&E (Vector Laboratories, #H-3502).

Biofilm formation assays

Biofilm formation assays were performed in 96-well flat-bottomed plates (VWR, 10861-562) coated with 100 μl of BSA or Fg (150 μg/ml) incubated overnight at 4°C. The various strains were grown as described above, and the inoculum was normalized to ~1 × 10^6 CFUs/ml. Cultures were then diluted (1:1000) into YPD, BHI, or human urine. Inoculum (100 μl) was incubated in the wells of the 96-well plate at 37°C for 48 hours while static.

Following the 48-hour incubation, the supernatant was removed from the plate and washed three times with 200 μl of 1× PBS to remove unbound fungi. Plates were fixed with 10% neutralizing formalin (Leica, 3800600) for 20 min followed by three washes with PBS containing 0.05% Tween-20 (PBS-T). Blocking solution [PBS with 1.5% BSA and 0.1% sodium azide (Acros Organics, 447811000)] was added to the plate for 1 hour at room temperature and then washed with PBS-T (3×). Biofilms were incubated with anti-*Candida* antibodies diluted into dilution buffer [PBS with 0.05% Tween-20 (VWR, M147-1L) and 0.1% BSA] for 2 hours. Plates were washed three times with PBS-T and incubated for 1 hour with IRDye 680 LT donkey anti-rabbit secondary antibody solution at room temperature and washed with PBS-T (3×). As a final step, the biofilms were visualized by scanning the plates using the Odyssey Imaging System (LI-COR Biosciences) and then analyzed with Image Studio software to obtain the fluorescence intensities (LI-COR version 5.2; Lincoln, NE).

BSA- or Fg-coated dishes and formation of fibrin fibers/nets

For these assays, no. 0 cover glass glass-bottom 35-mm petri dish with a 14-mm microwell (MatTek, P35G-0-14-C) was used. The dishes were coated with BSA (150 μg/ml) or Fg (150 μg/ml) overnight at 4°C. For fibrin fiber/nets formation, Fg and thrombin (Sigma-Aldrich, T6884-250UN) were thawed at 37°C. A total of 100 μl of Fg (0.5 mg/ml) in PBS was added into the microwell glass bottom, and then 10 μl of thrombin (2 U/ml) was added to polymerize Fg into fibrin. Dishes were incubated at 37°C for 1 hour and kept overnight at 4°C.

Visualization of biofilms and fungal-fibrin interactions

The various strains were grown as described above, and the inoculum was normalized to ~1 × 10^6 CFUs/ml in PBS. These cultures were then diluted (1:1000) into human urine; added to the BSA-, Fg-, or fibrin-coated dishes; and then were incubated at 37°C for 48 hours under static conditions. After incubation, dishes were then washed three times with 1× PBS to remove unbound fungi, and then dishes were fixed with 10% neutralizing formalin solution for 20 min and washed with 1× PBS three times. Dishes were blocked with blocking solution for an hour at room temperature as described above. Then, BSA- and Fg-coated dishes were incubated in primary antibodies, and fibrin-coated dishes were incubated with rabbit anti-*Candida* and goat anti-Fg antibodies. Incubation with the primary antibodies was done for 2 hours followed by three washes with PBS-T. Then, dishes were incubated for 1 hour with Alexa Fluor 594–labeled donkey anti-rabbit secondary antibody for BSA- and Fg-coated dishes and Alexa Fluor 594–labeled donkey anti-rabbit and Alexa Fluor 488–labeled donkey anti-goat antibodies for fibrin-coated dishes, followed by three washes with PBS-T. BSA- and Fg-coated dishes were visualized with a Zeiss inverted light microscope, and images were taken at different magnifications (10×, 20×, 40×, and 100×). Zen Pro and Fiji-ImageJ (*60*) software were used to analyze the images. For the fungal-fibrin interaction, fibrin-coated dishes were visualized by Nikon A1-R/Multi-Photon Laser Scanning Confocal Microscope, and images were analyzed by IMARIS Image Analysis software and ImageJ software (*60*).

Crystal violet staining

Following biofilm formation on Fg-coated microplate, the supernatant was removed, and the plate was incubated in 200 μl of 0.5% crystal violet for 15 min. Crystal violet stain was removed, and the plate was washed with water to remove the remaining stain. Plates were dried and then incubated with 200 μl of 33% acetic acid for 15 min. In another plate, 100 μl of the acetic acid solution was transferred, and absorbance values were measured via a plate spectrophotometer at 595 nm.

In vivo mouse model

Mice used in this study were ~6-week-old female WT C57BL/6 mice purchased from the Jackson Laboratory. Mice were subjected to transurethral implantation of a silicone catheter and inoculated as previously described (*35*). Briefly, mice were anesthetized by inhalation of isoflurane and implanted with a 6-mm-long silicone catheter (Braintree Scientific, SIL 025). Mice were infected immediately following catheter implantation with 50 μl of ~1 × 10^6 CFUs/ml in PBS, of one of the fungal strains introduced into the bladder lumen by transurethral inoculation. Mice were euthanized at 24 hpi by cervical dislocation after anesthesia inhalation, and the catheter, bladder, kidneys, spleen, and heart were aseptically harvested. Organs were homogenized, and catheters were cut into small pieces before sonication for fungal CFU enumeration. A subset of catheters was fixed for imaging as described below, and a subset of bladders was fixed and processed for IF and histology analysis as described below.

Catheter imaging and analysis

Harvested catheters were fixed for imaging via standard IF procedure as previously described (*34*). Briefly, catheters were fixed with formalin, blocked, washed with 1× PBS, and incubated with the appropriate primary antibodies overnight. Catheters were then incubated with secondary antibodies for 2 hours at room temperature. Catheters were washed with PBS-T and then a final wash with PBS. Catheters were visualized with the Odyssey Imaging System and then analyzed using color pixel counter from Fiji-ImageJ software (*60*). The number of pixels of each color was compared to the total number of pixels to identify percent coverage of the catheter.

Immunohistochemistry and H&E staining of mouse bladders

Mouse bladders were fixed in 10% formalin overnight, before being processed for sectioning and staining as previously described (*31*). Briefly, bladder sections were deparaffinized, rehydrated, and rinsed with water. Antigen retrieval was accomplished by boiling the samples in Na-citrate, washing in tap water, and then incubating in 1× PBS three times. Sections were then blocked [1% BSA and 0.3% Triton X-100 (Acros Organics, 21568-2500) in 1× PBS], washed in 1× PBS, and incubated with appropriate primary antibodies diluted in blocking buffer overnight at 4°C. Next, sections were washed with 1× PBS, incubated with secondary antibodies for 2 hours at room temperature, and washed once more in 1× PBS before Hoechst dye staining. Secondary antibodies for immunohistochemistry were Alexa Fluor 488 donkey anti-goat, Alexa Fluor 550 donkey anti-rabbit, and Alexa Fluor 650 donkey anti-rat. H&E stain for light microscopy was done by the corefacilities at the University of Notre Dame (ND Integrated Imaging core). All imaging was done using a Zeiss inverted light microscope and a Nikon A1-R/Multi-Photon Laser Scanning Confocal Microscope. Zen Pro, ImageJ software, and IMARIS Image Analysis software were used to analyze the images.

Measurement of *EFG1* and *ALS1* expression levels during *C. albicans* CAUTIs

Total RNA was extracted from infected and catheterized mouse bladders or biofilms with the QIAGEN RNeasy Kit (catalog no. 74004) or Zymogen RNA extraction kit (catalog no. R2071), respectively, and, subsequently, deoxyribonuclease I (DNase I)–treated. RNA was reverse-transcribed into cDNA via qScript cDNA synthesis kit (QuantaBio, catalog no. 101414); incubated for 5 min at 25°C, 30 min at 42°C, and 5 min at 85°C; and held at 4°C. qPCR was performed on QuantStudio 3 (Thermo Fisher Scientific) under the following conditions: $95°C^{5min}$ $(95^{15sec}, 60^{60sec})_{35\ cycles}$ $(95^{15sec}, 60^{60sec}, 95^{15sec})_{\ melt\ curve}$. Data were normalized using *ITS2* (internal transcribed spacer 2) as an internal housekeeping control gene (*60*) and WT as a sample calibrator and set the expression to 100% or 1. Data were analyzed via the ΔΔCt method. Primers are described in table S4.

Neutrophil analysis

Mouse bladders were harvested and minced into digestion buffer [Liberase (34 U/ml) and DNase1 (100 μg/ml) in Dulbecco's phosphate-buffered saline (D-PBS)]. Bladders were incubated for 1 hour in a heat block shaker at 37°C and 250 rpm and, every 15 min, were vortexed in high speed for 30 s. Digestion was arrested by the addition of D-PBS supplemented with 2% fetal bovine serum and 0.2 μM EDTA and passed through 40-μm cell strainers. Following a 20-min incubation in Fc block (BD Biosciences), cells were immunolabeled with the antibodies listed in table S5. Total cell counts in the bladder were determined on a BD LSRFortessa X-20 system cytometer (using DIVA software and analyzed by FlowJo software).

Statistical analysis

Data from at least three experiments were pooled for each assay. Two-tailed Mann-Whitney *U* tests were performed with GraphPad Prism 5 software (GraphPad Software, San Diego, CA) for all comparisons described in morphology, biofilm, CAUTI, neutrophils recruitment, qRT-PCR, and catheter coverage experiments. Values represent means ± SEM derived from at least three independent experiments ($*P < 0.05$; $**P < 0.005$; $***P < 0.0005$; $****P < 0.0001$; and ns, difference not significant).

Supplementary Materials

This PDF file includes:

Figs. S1 to S21
Tables S1 to S5
References

View/request a protocol for this paper from *Bio-protocol*.

REFERENCES AND NOTES

1. C. J. Nobile, A. D. Johnson, Candida albicans biofilms and human disease. *Annu. Rev. Microbiol.* **69**, 71–92 (2015).
2. C. Tsui, E. F. Kong, M. A. Jabra-Rizk, Pathogenesis of Candida albicans biofilm. *Pathog. Dis.* **74**, ftw018 (2016).
3. World Health Organization, WHO fungal priority pathogens list to guide research, development and public health action (World Health Organization, 2022).
4. F. L. Mayer, D. Wilson, B. Hube, *Candida albicans pathogenicity mechanisms*, *Virulence* **4**, 119–128 (2013).
5. D. S. Thompson, P. L. Carlisle, D. Kadosh, Coevolution of morphology and virulence in Candida species. *Eukaryot. Cell* **10**, 1173–1182 (2011).
6. S. M. Noble, B. A. Gianetti, J. N. Witchley, Candida albicans cell-type switching and functional plasticity in the mammalian host. *Nat. Rev. Microbiol.* **15**, 96–108 (2017).
7. P. E. Sudbery, Growth of Candida albicans hyphae. *Nat. Rev. Microbiol.* **9**, 737–748 (2011).
8. J. E. Nett, D. R. Andes, Contributions of the biofilm matrix to candida pathogenesis. *J Fungi (Basel)* **6**, 21 (2020).
9. K. E. Pristov, M. A. Ghannoum, Resistance of Candida to azoles and echinocandins worldwide. *Clin. Microbiol. Infect.* **25**, 792–798 (2019).
10. A. Flores-Mireles, T. N. Hreha, D. A. Hunstad, Pathophysiology, treatment, and prevention of catheter-associated urinary tract infection. *Top Spinal Cord Inj. Rehabil.* **25**, 228–240 (2019).
11. D. G. Maki, P. A. Tambyah, Engineering out the risk for infection with urinary catheters. *Emerg. Infect. Dis.* **7**, 342–347 (2001).
12. M. A. Rogers, L. Mody, S. R. Kaufman, B. E. Fries, L. F. Mc Mahon Jr., S. Saint, Use of urinary collection devices in skilled nursing facilities in five states. *J. Am. Geriatr. Soc.* **56**, 854–861 (2008).
13. A. Montoya, L. Mody, Common infections in nursing homes: A review of current issues and challenges. *Aging Health* **7**, 889–899 (2011).
14. J. F. Fisher, K. Kavanagh, J. D. Sobel, C. A. Kauffman, C. A. Newman, Candida urinary tract infection: Pathogenesis. *Clin. Infect. Dis.* **52Suppl 6**, S437–S451 (2011).
15. R. A. Garibaldi, J. P. Burke, M. L. Dickman, C. B. Smith, Factors predisposing to bacteriuria during indwelling urethral catheterization. *N. Engl. J. Med.* **291**, 215–219 (1974).
16. C. W. Norden, G. M. Green, E. H. Kass, Antibacterial mechanisms of the urinary bladder. *J. Clin. Invest.* **47**, 2689–2700 (1968).
17. J. W. Warren, Catheter-associated urinary tract infections. *Infect. Dis. Clin. North Am.* **11**, 609–622 (1997).
18. A. L. Flores-Mireles, J. S. Pinkner, M. G. Caparon, S. J. Hultgren, EbpA vaccine antibodies block binding of Enterococcus faecalis to fibrinogen to prevent catheter-associated bladder infection in mice. *Sci. Transl. Med.* **6**, 254ra127 (2014).

19. A. L. Flores-Mireles, J. N. Walker, T. M. Bauman, A. M. Potretzke, H. L. Schreiber, A. M. Park, J. S. Pinkner, M. G. Caparon, S. J. Hultgren, A. Desai, Fibrinogen release and deposition on urinary catheters placed during urological procedures. *J. Urol.* **196**, 416–421 (2016).
20. P. S. Guiton, T. J. Hannan, B. Ford, M. G. Caparon, S. J. Hultgren, Enterococcus faecalis overcomes foreign body-mediated inflammation to establish urinary tract infections. *Infect. Immun.* **81**, 329–339 (2013).
21. M. J. Andersen, C. K. Fong, A. A. la Bella, J. J. Molina, A. Molesan, M. M. Champion, C. Howell, A. L. Flores-Mireles, Inhibiting host-protein deposition on urinary catheters reduces associated urinary tract infections. *eLife* **11**, e75798 (2022).
22. A. L. Flores-Mireles, J. N. Walker, M. Caparon, S. J. Hultgren, Urinary tract infections: Epidemiology, mechanisms of infection and treatment options. *Nat. Rev. Microbiol.* **13**, 269–284 (2015).
23. J. N. Walker, A. L. Flores-Mireles, A. J. L. Lynch, C. Pinkner, M. G. Caparon, S. J. Hultgren, A. Desai, High-resolution imaging reveals microbial biofilms on patient urinary catheters despite antibiotic administration. *World J. Urol.* **38**, 2237–2245 (2020).
24. A. L. Flores-Mireles, J. N. Walker, A. Potretzke, H. L. Schreiber IV, J. S. Pinkner, T. M. Bauman, A. M. Park, A. Desai, S. J. Hultgren, M. G. Caparon, Antibody-based therapy for enterococcal catheter-associated urinary tract infections. *MBio* **7**, e01653-16 (2016).
25. P. S. Guiton, C. S. Hung, L. E. Hancock, M. G. Caparon, S. J. Hultgren, Enterococcal biofilm formation and virulence in an optimized murine model of foreign body-associated urinary tract infections. *Infect. Immun.* **78**, 4166–4175 (2010).
26. H. Bar-Yosef, N. Vivanco Gonzalez, S. Ben-Aroya, S. J. Kron, D. Kornitzer, Chemical inhibitors of Candida albicans hyphal morphogenesis target endocytosis. *Sci. Rep.* **7**, 5692 (2017).
27. H. Watanabe, M. Azuma, K. Igarashi, H. Ooshima, Relationship between cell morphology and intracellular potassium concentration in Candida albicans. *J. Antibiot.* **59**, 281–287 (2006).
28. J. E. Nett, E. G. Brooks, J. Cabezas-Olcoz, H. Sanchez, R. Zarnowski, K. Marchillo, D. R. Andes, Rat indwelling urinary catheter model of Candida albicans biofilm infection. *Infect. Immun.* **82**, 4931–4940 (2014).
29. J. E. Nett, R. Zarnowski, J. Cabezas-Olcoz, E. G. Brooks, J. Bernhardt, K. Marchillo, D. F. Mosher, D. R. Andes, Host contributions to construction of three device-associated Candida albicans biofilms. *Infect. Immun.* **83**, 4630–4638 (2015).
30. J. R. Gaston, M. J. Andersen, A. O. Johnson, K. L. Bair, C. M. Sullivan, L. B. Guterman, A. N. White, A. L. Brauer, B. S. Learman, A. L. Flores-Mireles, C. E. Armbruster, Enterococcus faecalis polymicrobial interactions facilitate biofilm formation, antibiotic recalcitrance, and persistent colonization of the catheterized urinary tract. *Pathogens* **9**, 835 (2020).
31. J. N. Walker, A. L. Flores-Mireles, C. L. Pinkner, H. L. Schreiber IV, M. S. Joens, A. M. Park, A. M. Potretzke, T. M. Bauman, J. S. Pinkner, J. A. J. Fitzpatrick, A. Desai, M. G. Caparon, S. J. Hultgren, Catheterization alters bladder ecology to potentiate Staphylococcus aureus infection of the urinary tract. *Proc. Natl. Acad. Sci. U.S.A.* **114**, E8721–E8730 (2017).
32. C. Colomer-Winter, J. A. Lemos, A. L. Flores-Mireles, Biofilm assays on fibrinogen-coated silicone catheters and 96-well polystyrene plates. *Bio Protoc.* **9**, e3196 (2019).
33. J. W. Weisel, R. I. Litvinov, Fibrin formation, structure and properties. *Subcell. Biochem.* **82**, 405–456 (2017).
34. C. Colomer-Winter, A. L. Flores-Mireles, S. Kundra, S. J. Hultgren, J. A. Lemos, (p)ppGpp and CodY promote *Enterococcus faecalis* virulence in a murine model of catheter-associated urinary tract infection. *mSphere* **4**, 10.1128/mSphere.00392-19, (2019).
35. M. S. Conover, A. L. Flores-Mireles, M. E. Hibbing, K. Dodson, S. J. Hultgren, Establishment and characterization of UTI and CAUTI in a mouse model. *J. Vis. Exp.* **e52892**, (2015).
36. M. Rousseau, H. M. S. Goh, S. Holec, M. L. Albert, R. B. Williams, M. A. Ingersoll, K. A. Kline, Bladder catheterization increases susceptibility to infection that can be prevented by prophylactic antibiotic treatment. *JCI Insight* **1**, e88178 (2016).
37. P. G. Pappas, C. A. Kauffman, D. R. Andes, C. J. Clancy, K. A. Marr, L. Ostrosky-Zeichner, A. C. Reboli, M. G. Schuster, J. A. Vazquez, T. J. Walsh, T. E. Zaoutis, J. D. Sobel, Clinical practice guideline for the management of candidiasis: 2016 update by the infectious diseases society of America. *Clin. Infect. Dis.* **62**, e1–e50 (2016).
38. L. J. Conway, E. J. Carter, E. L. Larson, Risk factors for nosocomial bacteremia secondary to urinary catheter-associated bacteriuria: A systematic review. *Urol. Nurs.* **35**, 191–203 (2015).
39. R. S. Shapiro, A. Chavez, C. B. M. Porter, M. Hamblin, C. S. Kaas, J. E. DiCarlo, G. Zeng, X. Xu, A. V. Revtovich, N. V. Kirienko, Y. Wang, G. M. Church, J. J. Collins, A CRISPR-Cas9-based gene drive platform for genetic interaction analysis in Candida albicans. *Nat. Microbiol.* **3**, 73–82 (2018).
40. S. M. Noble, S. French, L. A. Kohn, V. Chen, A. D. Johnson, Systematic screens of a Candida albicans homozygous deletion library decouple morphogenetic switching and pathogenicity. *Nat. Genet.* **42**, 590–598 (2010).
41. N. C. Gervais, A. A. La Bella, L. F. Wensing, J. Sharma, V. Acquaviva, M. Best, R. O. C. López, M. Fogal, D. Uthayakumar, A. Chavez, F. Santiago-Tirado, A. L. Flores-Mireles, R. S. Shapiro, Development and applications of a CRISPR activation system for facile genetic overexpression in Candida albicans.*G3 (Bethesda)*, 10.1093/g3journal/jkac301 , (2022).
42. M. Cavalheiro, M. C. Teixeira, Candida biofilms: Threats, challenges, and promising strategies. *Front. Med.* **5**, 28 (2018).
43. M. S. Rishpana, J. S. Kabbin, Candiduria in catheter associated urinary tract infection with special reference to biofilm production. *J. Clin. Diagn. Res.* **9**, DC11-13 (2015).
44. D. Keten, F. Aktas, O. Guzel Tunccan, M. Dizbay, A. Kalkanci, G. Biter, H. S. Keten, Catheter-associated urinary tract infections in intensive care units at a university hospital in Turkey. *Bosn. J. Basic Med. Sci.* **14**, 227–233 (2014).
45. N. H. S. Network. (Center for Disease Control, 2021).
46. P. Sepúlveda, J. L. López-Ribot, A. Murgui, E. Cantón, D. Navarro, J. P. Martínez, Candida albicans fibrinogen binding mannoprotein: Expression in clinical strains and immunogenicity in patients with candidiasis. *Int. Microbiol.* **1**, 209–216 (1998).
47. L. L. Hoyer, E. Cota, *Candida albicans* agglutinin-like sequence (Als) family vignettes: A review of Als protein structure and function. *Front. Microbiol.* **7**, 280 (2016).
48. P. S. Salgado, R. Yan, J. D. Taylor, L. Burchell, R. Jones, L. L. Hoyer, S. J. Matthews, P. J. Simpson, E. Cota, Structural basis for the broad specificity to host-cell ligands by the pathogenic fungus Candida albicans. *Proc. Natl. Acad. Sci. U.S.A.* **108**, 15775–15779 (2011).
49. J. Lin, S. H. Oh, R. Jones, J. A. Garnett, P. S. Salgado, S. Rusnakova, S. J. Matthews, L. L. Hoyer, E. Cota, The peptide-binding cavity is essential for Als3-mediated adhesion of Candida albicans to human cells. *J. Biol. Chem.* **289**, 18401–18412 (2014).
50. V. E. Glazier, EFG1, Everyone's favorite gene in Candida albicans: A comprehensive literature review. *Front. Cell. Infect. Microbiol.* **12**, 855229 (2022).
51. C. J. Nobile, E. P. Fox, J. E. Nett, T. R. Sorrells, Q. M. Mitrovich, A. D. Hernday, B. B. Tuch, D. R. Andes, A. D. Johnson, A recently evolved transcriptional network controls biofilm development in Candida albicans. *Cell* **148**, 126–138 (2012).
52. B. E. Glahn, O. Braendstrup, H. P. Olesen, Influence of drainage conditions on mucosal bladder damage by indwelling catheters. II. Histological study. *Scand. J. Urol. Nephrol.* **22**, 93–99 (1988).
53. E. M. Kojic, R. O. Darouiche, Candida infections of medical devices. *Clin. Microbiol. Rev.* **17**, 255–267 (2004).
54. M. Azmy, N. Nawar, M. Mohiedden, L. Warille, Electron microscopic assay of bacterial biofilm formed on indwelling urethral catheters. *J. Egypt. Soc. Parasitol.* **46**, 475–484 (2016).
55. C. Dunker, M. Polke, B. Schulze-Richter, K. Schubert, S. Rudolphi, A. E. Gressler, T. Pawlik, J. P. Prada Salcedo, M. J. Niemiec, S. Slesiona-Künzel, M. Swidergall, R. Martin, T. Dandekar, I. D. Jacobsen, Rapid proliferation due to better metabolic adaptation results in full virulence of a filament-deficient Candida albicans strain. *Nat. Commun.* **12**, 3899 (2021).
56. M. L. Wheeler, J. J. Limon, D. M. Underhill, Immunity to commensal fungi: Detente and disease. *Annu. Rev. Pathol.* **12**, 359–385 (2017).
57. J. V. Desai, M. S. Lionakis, The role of neutrophils in host defense against invasive fungal infections. *Curr. Clin. Microbiol. Rep.* **5**, 181–189 (2018).
58. S. Kenno, S. Perito, P. Mosci, A. Vecchiarelli, C. Monari, Autophagy and reactive oxygen species are involved in neutrophil extracellular traps release induced by C. albicans morphotypes. *Front. Microbiol.* **7**, 879 (2016).
59. V. Halder, C. B. M. Porter, A. Chavez, R. S. Shapiro, Design, execution, and analysis of CRISPR–Cas9-based deletions and genetic interaction networks in the fungal pathogen *Candida albicans*. *Nat. Protoc.* **14**, 955–975 (2019).
60. J. Schindelin, I. Arganda-Carreras, E. Frise, V. Kaynig, M. Longair, T. Pietzsch, S. Preibisch, C. Rueden, S. Saalfeld, B. Schmid, J. Y. Tinevez, D. J. White, V. Hartenstein, K. Eliceiri, P. Tomancak, A. Cardona, Fiji: An open-source platform for biological-image analysis. *Nat. Methods* **9**, 676–682 (2012).
61. C. Y. Turenne, S. E. Sanche, D. J. Hoban, J. A. Karlowsky, A. M. Kabani, Rapid identification of fungi by using the ITS2 genetic region and an automated fluorescent capillary electrophoresis system. *J. Clin. Microbiol.* **37**, 1846–1851 (1999).
62. F. C. Odds, A. J. Brown, N. A. R. Gow, *Candida albicans* genome sequence: A platform for genomics in the absence of genetics. *Genome Biol.* **5**, 230 (2004).
63. H. J. Lo, J. R. Köhler, B. DiDomenico, D. Loebenberg, A. Cacciapuoti, G. R. Fink, Nonfilamentous *C. albicans* mutants are avirulent. *Cell* **90**, 939–949 (1997).

Acknowledgments: We thank members of the laboratories of A.L.F.-M. and F.H.S.-T. for helpful suggestions and insightful comments. We give special thanks to M. G. Caparon for comments and S. Cole and the ND Integrated Imaging Facility for tissue processing and support during imaging. **Funding:** This work was supported by institutional funds from the University of Notre Dame (to A.L.F.-M. and F.H.S.-T.), NIH grants R01DK128805 (to A.L.F.-M., and M.J.A.) and R21AI171742 (to F.H.S.-T.), Arthur J. Schmitt Leadership Fellowship (A.A.L.B.), CIFAR Azrieli Global Scholar Award and Canadian Institutes of Health Research (CIHR) Project Grant PJT162195 (to R.S.S.), and NIH grant R35GM124594 (to C.J.N.). **Author contributions:** A.L.F.-M., and F.H.S.-T. designed the experiments. A.A.L.B., M.J.A., A.M., J.J.M., and P.V.S. performed the

studies. R.S.S., N.C.G., and L.W. designed and generated the adhesin mutant strain collection, the *ALS1* OE strain, and the clinical *efg1*Δ/Δ strains. C.J.N. generated the *efg1*Δ/Δ, *EFG1*-complemented, *als1*Δ/Δ, and *ALS1*-complemented strains. A.A.L.B., A.L.F.-M., and F.H.S.-T. wrote the paper. All authors contributed to editing the paper. **Competing interests:** C.J.N. is a cofounder of BioSynesis Inc., a company developing diagnostics and therapeutics for biofilm infections. All other authors declare that they have no competing interests. **Data and materials availability:** All data needed to evaluate the conclusions in the paper are present in the paper and/or Supplementary Materials.

Submitted 7 September 2022
Accepted 31 January 2023
Published 3 March 2023
10.1126/sciadv.ade7689